DISSERTATIONS IN
FORESTRY AND
NATURAL SCIENCES

Kalle Kuivalainen

Glossmeters for the measurement of gloss from flat and curved objects

Publications of the University of Eastern Finland
Dissertations in Forestry and Natural Sciences

UNIVERSITY OF
EASTERN FINLAND

KALLE KUIVALAINEN

Glossmeters for the measurement of gloss from flat and curved objects

Publications of the University of Eastern Finland
Dissertations in Forestry and Natural Sciences
No 44

Academic Dissertation
To be presented by permission of the Faculty of Science and Forestry for public examination in the Auditorium M100 in Metria Building at the University of Eastern Finland, Joensuu, on October, 14, 2011,
at 12 o'clock noon.

Department of Physics and Mathematics

Kopijyvä
Joensuu, 2011
Editors: Prof. Pertti Pasanen, Prof. Kai-Erik Peiponen,
Prof. Matti Vormanen

Distribution:
University of Eastern Finland Library / Sales of publications
P.O. Box 107, FI-80101 Joensuu, Finland
tel. +358-50-3058396
http://www.uef.fi/kirjasto

ISBN: 978-952-61-0524-6 (printed)
ISSNL: 1798-5668
ISSN: 1798-5668
ISBN: 978-952-61-0525-3 (pdf)
ISSNL: 1798-5668
ISSN: 1798-5676

Author's address:
University of Eastern Finland
Department of Physic and Mathematics
P.O.Box 111
FI-80101 JOENSUU
FINLAND
email: kalle.kuivalainen@uef.fi

Supervisor:
Professor Kai-Erik Peiponen, Ph.D.
University of Eastern Finland
Department of Physic and Mathematics
P.O.Box 111
FI-80101 Joensuu
FINLAND
email: kai.peiponen@uef.fi

Reviewers:
Jukka Räty, Ph.D., Docent
University of Oulu
CEMIS-Oulu, Kajaani
Kehräämöntie 7
P.O.Box 51
FI-87101 Kajaani
FINLAND
email: jukka.raty@oulu.fi

Jarkko J. Saarinen, Ph.D., Docent
Åbo Academi University
Laboratory of Paper Coating and Converting
Center of Functional Materials
Porthansgatan 3
FI-25000 Åbo/Turku
FINLAND
email: jarkko.j.saarinen@abo.fi

Opponents:
Professor Jouko Peltonen, Ph.D.
Åbo Academi University
Laboratory of Paper Coating and Converting
Center of Functional Materials
Porthansgatan 3
FI-25000 Åbo/Turku
FINLAND
email: jouko.peltonen@abo.fi

Professor Anssi Mäkynen, Dr. Tech.
University of Oulu
CEMIS-Oulu, Kajaani
Kehräämöntie 7
P.O.Box 51
FI-87101 Kajaani
FINLAND
email: anssi.makynen@oulu.fi

ABSTRACT

The focus of this thesis is the development of a diffractive optical element (DOE) based glossmeter (DOG). The original DOG and a new generation of DOGs are presented in this thesis. The experimental part of this thesis is divided into two sections, namely flat and curved surface gloss measurement. The flat surface inspection includes gloss measurement from cold-rolled stainless steel plates in a laboratory and on-line measurements in a printing line with new generations DOGs. A single sensor which can measure both gloss and surface roughness is also presented in this section. The measurements for this sensor were performed for a metal surface roughness standard. The DOGs for the curved surface were modified from the DOGs used for the flat surface and two statistical parameters for the curved surface gloss evaluation are presented here. The measurements for the curved surface DOGs were performed with unpainted and painted aluminium convex and concave sample series. The curved surface gloss measurement also includes one application where a latent fingerprint was detected on a ballpoint pen surface with the DOG.

PACS Classification: 42.25.Fx, 42.79.-e, 81.70.Fy
Universal Decimal Classification: 535.42, 62-408.64, 620.179.118, 621.7.015
INSPEC Thesaurus: gloss; surface roughness; optics; optical elements; diffraction; diffractive optical elements; optical sensors
Yleinen suomalainen asiasanasto: pinnat - - laatu; mittaus; mittausmenetelmät; mittauslaitteet; optiikka; optiset laitteet; optiset anturit

Preface

I would like to thank my supervisor Prof. Kai-Erik Peiponen for guidance through my studies. Moreover, I would like to thank the former head of department Dean Timo Jääskeläinen and the present head of department Prof. Pasi Vahimaa for giving me opportunity to work at the Department of Physics and Mathematics.

Special thanks belong to Ph.D. Antti Oksman for the contribution. In addition, I wish to thank the staff of Department of Physics and Mathematics. Also Prof. Patrick Gane, Ph.D. Kari Myller, Ph.D. Mikko Juuti and M.Sc. Carl-Mikael Tåg deserve thanks for their cooperation when preparing publications.

I want to express my thanks to reviewers Dos. Jukka Räty and Dos. Jarkko J. Saarinen for their careful reviews and comments, and Ph.D. Roy Goldblatt for the language correcting.

Finally, I want to thank my parents Kaarina and Antero for their love and support.

Joensuu 5 August, 2011 *Kalle Kuivalainen*

LIST OF PUBLICATIONS

This thesis consists of the present review of the author's work in the field of optical material inspection for flat and curved surfaces and the following selection of the author's publications:

I K. Kuivalainen and A. Oksman and M. Juuti and K. Myller and K.-E. Peiponen, "Advanced glossmeters for industrial applications," *Opt. Rev.* **17,** 248–251 (2010).

II A. Oksman and K. Kuivalainen and C.-M. Tåg and M. Juuti and R. Mattila and E. Hietala and P.A.C. Gane and K.-E. Peiponen, "Diffractive optical element-based glossmeter for the online measurement of normal reflectance on a printed porous coated paper," *Opt. Eng.* **50,** 043606 (2011).

III K. Kuivalainen and A. Oksman and K.-E. Peiponen, "Definition and measurement of statistical gloss parameters from curved objects," *Appl. Opt.* **49,** 5081–5086 (2010).

IV K. Kuivalainen and K.-E. Peiponen and K. Myller, "Application of a diffractive element-based sensor for detection of latent fingerprints from a curved smooth surface," *Meas. Sci. Technol.* **20,** 077002 (2009).

Throughout the overview, these papers will be referred to by Roman numerals.

AUTHOR'S CONTRIBUTION

The author has done the major part of the experimental work in papers **I**, **III-IV** and has done part of the paper **II** experimental work. The author has participated in writing papers **II** and **IV** and has largely written papers **I** and **III**.

Contents

1 Introduction

Surface quality inspection has become important in a variety of fields such as the metal, plastic, paper and printing industries because it is an effective way to decrease production costs [1]. Optical measurement methods, in particular, are widely used for surface quality inspection since the optical measurements do not destroy the measurement objects [1]. Two commonly used parameters for surface appearance evaluation are surface roughness and gloss. The inspection of the gloss is the main focus of this thesis. In addition, the theory and measurement of surface roughness is considered in this thesis because gloss and surface roughness are closely connected to each other.

Gloss has a substantial effect on surface appearance [2–6] and describes the power of the surface to reflect light specularly. According to Hunter and Harold [5] gloss is divided into six different categories. The most commonly used gloss type is specular gloss. The inspection of specular gloss is complicated because the incident angle of the beam, polarization of the light, complex refractive index of the medium, surface roughness and color have an effect on the gloss [2–6]. In daily life, gloss is inspected by the eye, and therefore several psychophysical studies have been done where visual inspection and glossmeters readings are compared [7–9].

There are several standards for specular gloss inspection. The most widely used standards are the American Society of Testing and Materials (ASTM) D523 [10] and the International Standards of Organization (ISO) 2813 [11]. In general, conventional glossmeters [5,12–14] have been designed according to the ASTM D523 and ISO 2813 standards. However, problems occur if the inspected surface is non-planar, small, curved or moving vertically in the plane of light incidence (normal to the surface plane). A partial solution for these measurement problems is a diffractive optical element (DOE) based glossmeter (DOG) [6, 15–17]. The measurement of the gloss

has been widely studied, but there are two fields which have been rather briefly studied, on-line gloss inspection and gloss measurement of curved objects. Both subjects are considered in this thesis.

The DOG is a multipurpose glossmeter and it has been used for the specular gloss measurement of different objects such as plastics [18, 19], pharmaceutical tablets [20, 21], metals [22–24], prints and papers [25–30], wood [31] and nanocarbon surfaces [32]. DOG has also been used for contrast gloss measurements on the prints [33, 34], the visibility map measurement of prints [35] and gloss reference surface uniformity inspection [36]. The DOE, which is used in the DOG, is an important part of several sensors which have been used in the quality inspection of paper and print [37–40], pharmaceutical tablets [41, 42], wood inspection [43–46], the complex refraction index measurements of liquids [47], the refractive index change measurement of liquids [48], float glass thickness measurement [49], the quality inspection of punches [50, 51], human plasma fibrinogen sensing on a titanium surface [52, 53], ceramic product inspection [54] and local curvature and roughness measurement [55].

The main focus of this thesis is the development of the DOGs and specular gloss measurement from flat and curved objects. Chapter 2 considers the theory of specular gloss and factors related to specular gloss. Also, the statistical specular gloss parameters for a flat [24] and a curved surface are presented in chapter 2. The presented statistical parameter, average gloss G_{ave} and gloss variation G_{var} are useful for the estimation of the gloss of both convex and concave surfaces. The original DOG and the new generations of DOGs, namely μDOG 1D, μDOG 2D and the handheld wireless glossmeter (HWDOG) for flat surface inspection are presented in chapter 3. Chapter 3 also considers cold-rolled metal plate inspection by means of the HWDOG and μDOG 2D, and on-line glossmeter (μDOG 1D) laboratory tests, and on-line measurement in the printing line. In addition, a novel single sensor which can detect both gloss and surface roughness is presented in this chapter. Chapter 4 considers the gloss measurements of convex and concave

aluminium samples. These measurements were performed with two glossmeters. One was developed from the original DOG and the second from the HWDOG. In addition, an application where a latent fingerprint is reconstructed on a ballpoint pen is presented in chapter 4. All gloss measurements in this thesis consider specular gloss, hence the term ”gloss” means specular gloss.

2 Definition of gloss

Gloss is a useful parameter in the evaluation of the surface quality of products and is a widely used parameter for evaluating surface appearance [2, 4–6]. Gloss is a widely used parameter to quantify and categorize different materials: for example, the evaluation of the surface quality of metals [22, 23, 56], plastic and composite materials [18, 19, 57, 58] and dental materials [59]. In the printing industry gloss inspection is a daily task because high gloss is a major indicator of high print quality [60–67]. Another field of industry where gloss inspection has been used is the food industry, where it is possible to find spoiled food by means of gloss inspection [68–74]. Specular gloss and subjects having an effect on the specular gloss are considered in this chapter. The problems of measuring specular gloss are also discussed in this chapter.

2.1 SPECULAR GLOSS

Specular gloss describes the surface capability to reflect light in a specular direction. When light reflects in the specular direction the illumination and reflection angles are the same. If the surface is ideally smooth, all of the reflected light is in the specular direction. If the shape of the surface is irregular, part of the light is reflected in the specular direction and part of the illumination light is reflected in the diffuse direction. The specular and diffuse reflection of light is illustrated in Fig. 2.1.

The measurement of specular gloss for a planar surface is defined according to the American Society of Testing Materials (ASTM) D523 [10] and the International Standard of Organization (ISO) 2813 [11]. According to these two international standards, the illuminating angle i.e. angle between the surface normal and incoming light is 20°, 60° or 85° depending on the inspected surface where 20° is used for high gloss, 60° for semigloss and 85° is used for

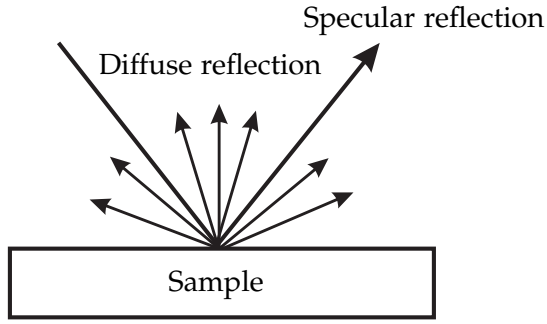

Figure 2.1: Specular and diffuse reflection of a planar surface.

low gloss samples [4, 5, 10, 11]. In the standards, the light source is defined and gloss also depends on the illumination. Light source is typically a halogen lamb which produces white light. Most conventional glossmeters have been designed according to these standards. However, there are some problems in using conventional glossmeters. The measurement area of the conventional glossmeters is relatively large, approximately 1 cm^2. However, measurement area depends on the measurement geometry. In general, conventional glossmeters have been designed for contact measurement, which can be a problem if the inspected surface is fragile. Gloss standards also assume that many different measurement geometries are needed, which is a problem when measurement results with the different geometries are compared. There are also other similar standards, for specular gloss measurement, for example ISO 8254-1, ISO 8254-2, ISO 8254-3. [75–77]. Both ASTM D523 and ISO 2813 standard are general standards for the specular gloss measurement which were defined for several measurement geometries. Standard in Refs. [75–77] were defined only for one measurement geometry. The specular gloss standard defines light source and the shape of the light beam which is collimated or converging. The light source of ASTM D523 and ISO 2813 is illuminant C and it simulates average daylight. The light source in ISO 8254-1, ISO 8254-2, ISO 8254-3 is illuminant A and it is an average incandescent light source. The light sources have an effect on gloss readings. If the same sample is

measured with different glossmeters which have a different light sources, the glossmeter which uses illuminant A gives a higher gloss reading than the glossmeter which uses illuminant C if the color of a sample is red. Because the illuminant A emits more red light than the illuminant C. The list of all international gloss measurement standards can be found in [6].

These international standards assume that the inspected surface is planar and the illumination angle is 20° or larger. Problems occur if the surface is non-planar, moving vertically, small or curved. If the surface is smooth and planar, all reflected light on the surface is reflected in the same direction. The measurement of convex and concave surfaces is problematic with a conventional glossmeter because the diameter of the collimate light beam is usually approximately 10 mm, where the reflected light rays of the convex and concave surface are not parallel. The specular reflection of the convex and concave surface is presented in Fig. 2.2.

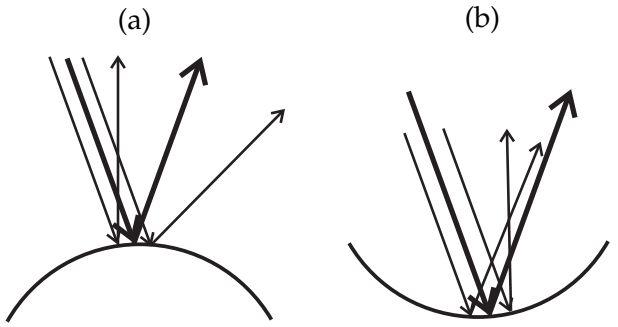

Figure 2.2: Specular reflection in (a) convex and (b) concave surface. The darkest arrow describes the optimal reflection.

The specular gloss GU is defined as the ratio between the measured irradiance of the sample and the gloss reference as follows:

$$GU = \frac{I_{\text{sample}}}{I_{\text{reference}}} \times 100, \tag{2.1}$$

where I_{sample} is the irradiance of the sample and $I_{\text{reference}}$ the irradiance of gloss reference, which is black glass with the refractive index n=1.567 and its gloss reading is defined to be equal 100 GU.

2.2 CONVENTIONAL GLOSSMETERS

The term conventional glossmeter refers a glossmeter which has been designed precisely, according to international standards [10, 11, 75–77]. The light source of the conventional glossmeters is a white light source with measurement angles of 20° or larger. The commonly used measuring geometries are 20°, 45°, 60°, 75° and 85°. Typically used gloss measuring geometries and the measurement principle are presented in Fig. 2.3. The geometry used depends on the material and glossiness of the inspected surface which is assumed to be flat. The principle of measuring with the conventional glossmeter is simple. The inspected surface is illuminated by the light source at an angle and the light reflected from the surface is measured by a detector located at the same but opposite angle. The problems and limitations of conventional glossmeters have been discussed in [5, 6, 15].

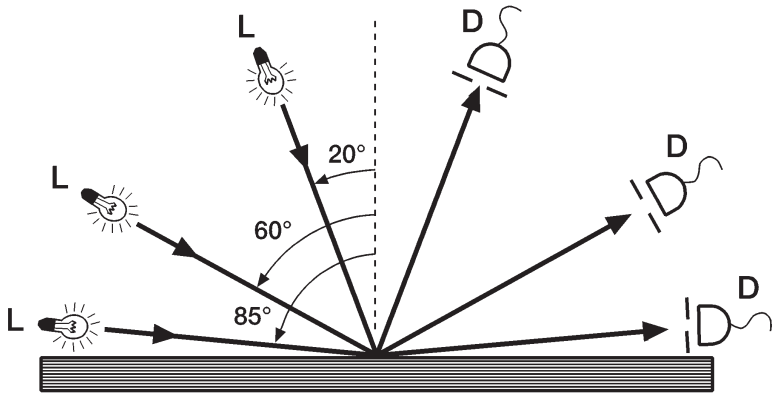

Figure 2.3: Gloss measuring geometries for 20°, 60°, 85°. L= light source and D = detector.

2.3 GLOSS REFERENCE

According to ISO 2813 and ASTM D523 [10,11], the gloss reference used is highly polished black glass with a refractive index of 1.567 for the sodium D line, i.e. at the wavelength 589 nm. The gloss standard is theoretical because there is no black glass with a refractive index of exactly 1.567 [78]. For the highly polished black glass, the gloss value is defined as 100 gloss units GU. However, there are problems with the black glass gloss standards, such as the gloss standards not being uniform. The problems of the gloss standards have been discussed in [13,14,36,78,79].

2.4 DEFINITION OF STATISTICAL GLOSS PARAMETERS

Several statistical gloss parameters have been established to estimate gloss, which are analogous to the surface roughness parameters. Statistical parameters are needed because traditional gloss is more or less a mean gloss level and the evaluation of gloss cannot be characterized using only mean gloss [61]. Statistical parameters for a planar surface and for specular gloss have been presented in [24] and statistical parameters for contrast gloss have been presented

in [33]. Moreover, there are a number of studies in which the perception of gloss and lightness for other image statistic parameters, such as skewness, has been compared [80,81]. For a curved surface, i.e. convex and concave, the statistical gloss parameters differ from the planar surface parameters because the measurement path of the gloss is a curved path P. Statistical gloss parameters for a curved surface are represented in **Paper III**. In this section statistical gloss parameters are represented both for planar and curved surfaces.

2.4.1 Statistical gloss parameters for a planar surface

The mean gloss G_{mean} for a planar surface is defined in two-dimensional case as follows

$$G_{\text{mean}} = \langle G(x,y) \rangle = \frac{1}{A} \int \int_A G(x,y) \text{dxdy}, \tag{2.2}$$

where A is the measurement area, and $G(x,y)$ the gloss as a function of location in the Cartesian coordinate. There are two different parameters for the estimation of gloss variation, namely the average and the rms gloss, which are defined as follows

$$G_{\text{a}} = \frac{1}{A} \int \int_A |G(x,y) - \langle G(x,y) \rangle| \text{dxdy} \tag{2.3}$$

and

$$G_{\text{q}} = \sqrt{\frac{1}{A} \int \int_A |G(x,y) - \langle G(x,y) \rangle|^2 \text{dxdy}}, \tag{2.4}$$

where $\langle G(x,y) \rangle$ is the mean gloss in a manner that $G(x,y)$ has a minimum variance. These equations are defined in the two-dimensional case for the gloss measurement of an area A. It is, however, possible to simplify these equations for a one-dimensional case if the measurement has been made along a straight line. There are also other parameters for gloss evaluation such as slope parameters, autocorrelation and the power spectral density function of the gloss. The slope parameters give a direction where the gloss gradient is strongest. The autocorrelation function quantifies similarities of the gloss profile in a lateral direction and the power spectral density function describes periodicity in the spatial frequency plane [24].

2.4.2 Statistical gloss parameters for a curved surface

The statistical gloss parameter definitions for a planar surface are rather straightforward and based on the assumption of the planarity of the object surface [24]. However, there are situations where it is impossible to evaluate gloss readings using the abovementioned parameters for a planar surface. The definitions for statistical gloss parameters for a curved surface are based on the assumption that the gloss profile is measured along a curved path P in which the concept of a line integral is essential. If the light beam is infinitely thin, then the probed location on the curved surface can be considered apparently flat, and the gloss measurement is possible. If the curved object is sufficiently regular such as a cylinder, it is usually possible to use a simple measurement path, such as a rectilinear line or the arc of a circle. For a curved surface, the average gloss G_{ave} is defined as follows:

$$G_{\text{ave}} = \frac{1}{L}\int_P G(s)\text{ds} = \frac{1}{L}\int_a^b G(r(t))\Big|\frac{dr(t)}{dt}\Big|\text{dt}, \tag{2.5}$$

where $ds = |dr|$ is an infinitesimal line segment along path P, G denotes the gloss reading along the path, L is the length of the path, and a and b are the initial and final points of the measurement path, respectively. The equality on the right-hand side in Eq. 2.5 holds under the assumption of a parametric presentation for a rectifying and piecewise smooth measurement path, which is given as a function of parameter t.

Gloss variation G_{var} or gloss mottling is defined as follows:

$$\begin{aligned} G_{\text{var}} &= \frac{1}{L}\int_P |G(s) - G_{\text{ave}}|\text{ds} \\ &= \frac{1}{L}\int_a^b |G(r(t)) - G_{\text{ave}}|\Big|\frac{dr(t)}{dt}\Big|\text{dt}. \end{aligned} \tag{2.6}$$

The equations 2.5 and 2.6 have been defined along a curved path P. However, in two-dimensional case Eqs. 2.5 and 2.6 can be used because the gloss parameters of each measurement path are calculated separately and the final result is an average of all the individ-

ual measurement points which are measured along a measurement path.

2.5 SURFACE ROUGHNESS

Surface roughness has a significant effect on light scattering and therefore has an effect on gloss [63,82–85]. Gloss and surface roughness have a negative correlation [6, 86]. In general, high surface roughness means low gloss and *vice versa*. However, this assumption is not valid in every situation because it is possible that two different surfaces have similar root-mean-squre (rms) surface roughness but the gloss reading is different [3]. The surface roughness depends also measurement length or area.

The measurement techniques of surface roughness can be divided into two different categories, namely contact or noncontact measurement [1, 85, 87]. Contact measurement is based on a diamond stylus measurement where the diamond stylus is scanned over the measured surface along a straight line [1, 85, 88, 89]. The problem with diamond stylus measurements is that fragile and porous materials such as pharmaceutical tablets can be destroyed during the measurement. A non-contact surface roughness measurement is based on some phenomenon of optics such as specular reflection [90], scattering of light [91–98] from an inspected surface, or just simply using a laser stylus and triangulation [1, 99].

There are several parameters for the evaluation of surface roughness since one parameter is normally insufficient for the evaluation. The most common parameters for this evaluation are average surface roughness R_a and root-mean-square (rms) roughness R_q which are defined in a one-dimensional case as follows [1]

$$R_\mathrm{a} = \frac{1}{L}\int_o^L |f(x) - \langle f(x)\rangle|\mathrm{dx}, \tag{2.7}$$

and

$$R_\mathrm{q} = \sqrt{\frac{1}{L}\int_o^L |f(x) - \langle f(x)\rangle|^2\mathrm{dx}}, \tag{2.8}$$

where L is the measurement length, $f(x)$ the surface profile along a thin line and $\langle f(x) \rangle$ a mean line chosen so that $f(x)$ has a minimum variance. The definition of the surface roughness parameters in a two-dimensional case is rather similar when the integration is over the measurement area.

2.5.1 Speckle pattern

When a rough surface is illuminated with coherent laser radiation the light is scattered from the sample surface and produces an interference pattern which is a so-called speckle pattern. The speckle pattern consists of dark areas when destructive interference occurs and bright areas when constructive interference occurs [100, 101]. Two types of speckle patterns exist, namely a static speckle pattern which is valid when the object does not move and the laser is stable, and a dynamic speckle pattern which appears when the interference pattern changes as a function of the time [102].

The speckle pattern is useful for surface roughness inspection [94–97, 100, 101]. The technique presented in [94–97, 100, 101] is based on the calculation of the angular speckle correlation between two speckle patterns which are obtained from the same location of the inspected surface with two slightly different illumination angles. Correlation C is calculated from the formula as follows:

$$C(I_1, I_2) = \frac{\sum_{x,y=1}^{M,N}(I_1(x,y) - \bar{I}_1)(I_2(x,y) - \bar{I}_2)}{\Big[\sum_{x,y=1}^{M,N}((I_1(x,y) - \bar{I}_1)^2 \sum_{x,y=1}^{M,N}((I_2(x,y) - \bar{I}_2)^2\Big]^{\frac{1}{2}}}, \quad (2.9)$$

where $I_1(x,y)$ and $I_2(x,y)$ are the intensities of the speckle pattern and $\bar{I}_1$ and $\bar{I}_2$ the mean intensities of the speckle patterns. If the surface roughness height statistic follows a Gaussian distribution, it is possible to calculate the rms-surface roughness by using the following equation:

$$C(\delta\theta) = \exp\Big[-\sigma^2\Big(\frac{4\pi \sin\theta}{\lambda}\Big)^2 \delta\theta^2\Big], \quad (2.10)$$

where θ is the illumination angle, $\delta\theta$ the rotation angle, σ the rms-surface roughness and λ the wavelength of the laser. The analysis of the speckle pattern also has other advantages in the field of optical measurement such as measuring the mean particle size of bulk powder [103, 104], bioflow measurement [105], local deformation measurement of a tablet surface [106] and blood flow measurement [107]. More detailed review of speckle patterns measurement techniques can be found [100–102]. In this thesis a measurement setup is presented which is able to measure both gloss and surface roughness from the same location.

2.6 REFRACTIVE INDEX

Refractive index is defined by the ratio between the speed of light in a vacuum and in a medium as follows:

$$n(\omega) = \frac{c}{v(\omega)}, \tag{2.11}$$

where c is the speed of the light in the vacuum and $v(\omega)$ is the speed of the light in the medium. For a non-absorbing medium the refractive index is defined by the following equation [108]:

$$n(\omega) = \sqrt{\epsilon_r(\omega)\mu_r(\omega)}, \tag{2.12}$$

where $\epsilon_r(\omega)$ is the relative permittivity and $\mu_r(\omega)$ the magnetic permeability of the medium. For materials which absorb light, the refractive index is complex and is defined as follows:

$$\tilde{n}(\omega) = n(\omega) - \mathrm{i}\kappa(\omega), \tag{2.13}$$

where $n(\omega)$ is the real part and $\kappa(\omega)$ is the imaginary part of the complex refractive index. Materials have an intrinsic refractive index which depends on the wavelength of the light. Refractive indexes can be found in the literature for different materials, e.g. for solid materials [109].

2.7 FRESNEL'S EQUATIONS

Specular reflectance for a smooth surface can be calculated using Fresnel's equations, which describe the behaviour of the light when it is reflected from the surface. Fresnel equations for reflectance are defined for transverse electric field (TE) polarized light R_{TE} and transverse magnetic field (TM) polarized light R_{TM} as follows [108]:

$$\begin{aligned} R_{\mathrm{TE}} &= r_{\mathrm{TE}} r_{\mathrm{TE}}^{*} \\ &= \left| \frac{n_1 \cos\theta - \left[(n_2 - \mathrm{i}\kappa_2)^2 - n_1^2 \sin^2\theta \right]^{\frac{1}{2}}}{n_1 \cos\theta + \left[(n_2 - \mathrm{i}\kappa_2)^2 - n_1^2 \sin^2\theta \right]^{\frac{1}{2}}} \right|^2 \end{aligned} \tag{2.14}$$

and

$$\begin{aligned} R_{\mathrm{TM}} &= r_{\mathrm{TM}} r_{\mathrm{TM}}^{*} \\ &= \left| \frac{(n_2 - \mathrm{i}\kappa_2)^2 \cos\theta - n_1 \left[(n_2 - \mathrm{i}\kappa_2)^2 - n_1^2 \sin^2\theta \right]^{\frac{1}{2}}}{(n_2 - \mathrm{i}\kappa_2)^2 \cos\theta + n_2 \left[(n_2 - \mathrm{i}\kappa_2)^2 - n_1^2 \sin^2\theta \right]^{\frac{1}{2}}} \right|^2 , \end{aligned} \tag{2.15}$$

where r_{TE} and r_{TM} are reflection amplitudes for TE- and TM-polarized light, * denotes complex conjugate, n_1 is the refractive index of the medium 1, θ the angle of the incidence, n_2 and κ_2 are real and imaginary part of the refractive indexes of the medium 2, respectively.

2.8 OTHER TYPES OF GLOSS

As mentioned previous, the concept of the gloss consist total six different gloss types. Specular gloss was discussed earlier in this chapter. Sheen is almost the same as specular gloss. The difference between the two is that the incident angle of sheen is 88° whereas in specular gloss it can change. Sheen is generally used for low gloss samples [5]. Haze, or the absence of bloom, is scattered light which produces a cloudy appearance adjacent to a bright beam of reflected

light. Contrast gloss is the ratio between specularly and diffusely reflected light and identifies a difference in the visual appearance between two different surfaces having the same specular gloss [33]. Distinctness of image gloss describes the sharpness of specularly reflected light and surface uniformity gloss describes freedom from visible nonuniformities such as texture.

3 Development of diffractive element based glossmeters for flat object inspection

A glossmeter which was based on the diffractive optical element (DOE) was presented in 2003 [18]. The DOE which is a crucial part of DOG was used for the first time in the middle of the 1990s [110]. The diffractive optical element based glossmeter (DOG) has since been used for many different applications. The final results of the development of the DOG are its commercial prototypes, namely μDOG 1D, μDOG 2D and the handheld wireless glossmeter (HW-DOG) (MGM-devices Ltd, Joensuu, Finland). The main focus in this chapter is the development of the DOG from the original laboratory version to the off-line and on-line DOGs. The properties and advantages of the original DOG and the new generation of DOGs are presented in this chapter. In addition, one solution is presented for a sensor which is able to measure both the gloss and surface roughness from the same location. New DOGs are presented in **Paper I** and the on-line glossmeter and on-line gloss measurements are presented in **Papers I** and **II**.

3.1 ORIGINAL DIFFRACTIVE OPTICAL ELEMENT BASED GLOSSMETER

The original old generation diffractive optical element based glossmeter consists of a monochromatic light source namely a HeNe laser with a wavelength of 632.8 nm, lenses, a *x*-*y*-*z*-translation stage and the DOE. A schematic diagram of the DOG is presented in Fig. 3.1. The principle of DOG measurement is the following. The collimated laser beam is focused using a lens on the sample surface.

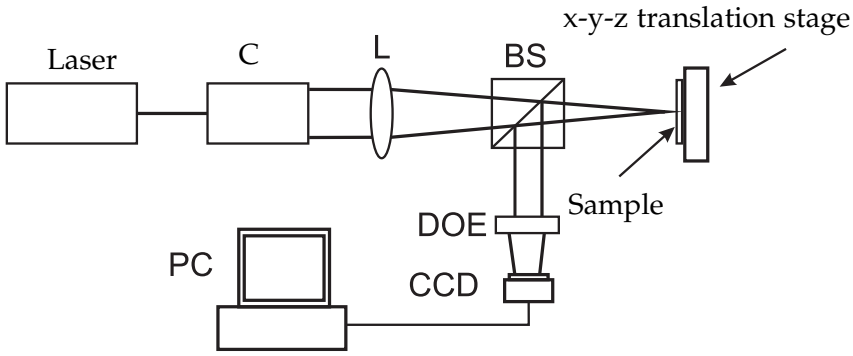

Figure 3.1: Schematic diagram of the original DOG. BS = beam splitter, L = focusing lens, C = collimating optics, DOE = diffractive optical element, CCD = charge-coupled device, PC = Personal computer.

The specular reflection of the sample is guided through to the beam splitter (BS) to the DOE. The DOE reconstructs a 4×4 light spot matrix in its focal plane (f=100 mm) where the detector is located. The detector is a CCD- or CMOS-camera. The focus size is possible to choose freely typically between the 10 to 100 μm at $1/e$-level. The aperture size of the DOE is 4 mm $\times$ 4 mm. The DOE was calculated using Rayleigh-Sommerfield diffraction integral [111] and was produced using electron beam lithography. The imaging properties of the DOE follow the laws of hologram imagery [112,113]. The imaging properties of the DOE have been presented in [6,26,37,42,44,45]. The sample is scanned with the aid of the *x*-*y*-*z*-translation stage.

It has previously been shown that DOG has several advantages. The DOG can detect small gloss readings a nano-carbon surface [32] and small gloss variations on printed products [34]. The sensitivity of the DOG is relatively good 0.001 gloss unit (G) (see gloss definition in Eq. 3.2) [32]. The repeatability of the DOG is approximately 0.3 % which was measured five times from a high gloss metal plate [6]. The DOG's normal incidence of light allows it to measure complex objects and the effect of the polarization and vertical movement of the sample are not significant [6].

The DOE has been designed for a monochromatic light source and a particular wavelength. The main advantages of the DOE are

that both the amplitude and phase information concerning scattered light affect the reconstructed image. The DOE also reduces the noise of the speckle pattern in the direction of specular light reflection on the detector plane and acts as a spatial filter [6, 16]. The DOE reconstructs a large number of light spots (16), which increases the statistical repeatability and reliability of the measurements. The focal length of the DOE was 100 mm. However, it is possible to design and fabricate a DOE where focal length is smaller, such as 20 mm, which enables the development of small devices, as shown in **papers I-III** and Ref. [6].

The light source of the DOG is a monochromatic HeNe laser whereas in conventional glossmeters it is a white light source. The monochromatic light source is used because it is free of the effect of fluctuations of the spectral band of a white light source. Using laser light will give better stability, a longer lifetime of a light source and possibility to use a collimated beam [6].

The data analysis of the DOG is based on the calculating the total irradiance of the DOE image by means of the following equation:

$$I = \frac{1}{nm} \sum_{i}^{n} \sum_{j}^{m} I_{ij}, \tag{3.1}$$

where I_{ij} is the irradiance detected by the (i,j)th element of the detector array. Gloss G is defined in the case of DOG as follows:

$$G = \frac{I_{\text{sample}}}{I_{\text{ref}}} \times 100, \tag{3.2}$$

where I_{sample} and I_{ref} are irradiances of the sample and gloss reference calculated by Eq. 3.1. Eq. 3.2 is analogous to the standardized specular gloss (Eq. 2.1).

A useful parameter for evaluating surface quality by using DOG is visibility. Visibility provides information on surface roughness and surface texture [5], such as finishing marks, whereas gloss contains information about surface roughness and the refractive index [22, 35].

3.2 NEW GENERATION OF DOGS

The new generation of the DOGs consists of three different glossmeters, namely μDOG 1D, μDOG 2D and HWDOG. These glossmeters have been developed for different purposes. The μDOG 1D is a one-dimensional on-line glossmeter designed for on-line gloss inspection in a printing house. The μDOG 2D is a scanning glossmeter designed to measure gloss from areas of few square millimeters to several square centimeters. It was designed only for laboratory use or industrial off-line use. The HWDOG was designed for rapid gloss inspection in a laboratory and off-line surface quality testing in industry. These glossmeters and the measurement results have been introduced in **Papers I** and **II**.

3.2.1 μDOG 1D and μDOG 2D

μDOG 1D and μDOG 2D have the same construction but different fields of application. A schematic diagram of the μDOG 1D and the μDOG 2D is shown in Fig. 3.2. The measurement principle of both glossmeters is quite similar to the original DOG. The main differences between the DOG and μDOGs are that the construction of the optics in the μDOGs is simpler than in the DOG and the detector in the μDOGs is a photodiode which provides faster data processing. The optics of these gauges is much more tightly packed than the original laboratory version of the DOG. The light source of the μDOGs is a semiconductor laser operating at the wavelength of 635 nm (P = 5 mW). The angle of incidence of both glossmeters is 0° i.e. the surface normal direction. The aperture size of the DOE is 2 mm $\times$ 2 mm and the focal length is 20 mm. The measured laser spot size at the $1/e$- level of the maximum irradiance of the light beam in μDOG 1D is about 40 μm and in μDOG 2D about 30 μm.

μDOG 1D consists of only a measurement head. Depending on the applications it is used, the stand of the μDOG 1D must be designed and built separately. The measurement data of the μDOG 1D are transferred from the gauge to the computer through a network and the sampling rate is approximately 1250 measurements

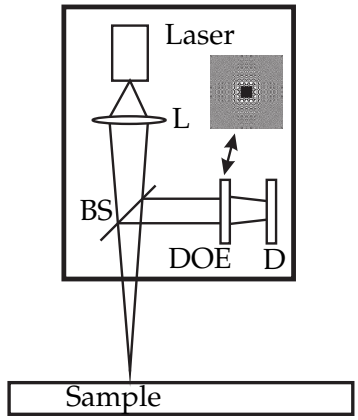

Figure 3.2: Schematic diagram of the μDOG 1D and μDOG 2D. BS = beam splitter, L = focusing lens, DOE = diffractive optical element, D = detector (a single cell photodiode). The aperture of the DOE is showed in the inset.

per second. The measurement signal is the one-dimensional gloss profile of the object. The gloss profile can be presented as a gloss matrix if the measurement sample is periodic, as in a printing line. The gloss matrix is a visual presentation where the gloss profile is cut in pieces thus one piece includes the measurement points of one printed sheet. These pieces are connected into one matrix which is called as a gloss matrix. The signal-to-noise ration (SNR) of the internal reflections is approximately 43 dB depending on the optical power of the laser used. The internal reflections in both μDOG 1D and μDOG 2D are reduced by using apertures.

μDOG 2D consist of two parts: a stable optical bench and the measurement head. The measurement data of μDOG 2D is transferred from the gauge to the computer through an USB cable. The measurement data is collected in the matrix and it is possible to calculate statistical gloss parameters [24] and obtain a gloss map. This glossmeter enables the measurement of samples with different thicknesses because it has a screw for adjusting the surface of the object at the focal length of the glossmeter.

3.2.2 Handheld wireless glossmeter (HWDOG)

The handheld wireless glossmeter (HWDOG) was designed for a rapid product quality inspection in a laboratory and for off-line industrial use. The HWDOG is a contact glossmeter and therefore the measurement of fragile objects is problematic. The light source is a semiconductor laser (P = 0.8 mW) operating at the wavelength 635 nm and the detector is a photodiode. The construction of optics differs from the μDOG 1D and the μDOG 2D because the incident angle of the laser beam is 6°. The focus size at $1/e$-level is 30 μm. A schematic diagram of the HWDOG is shown in Fig. 3.3.

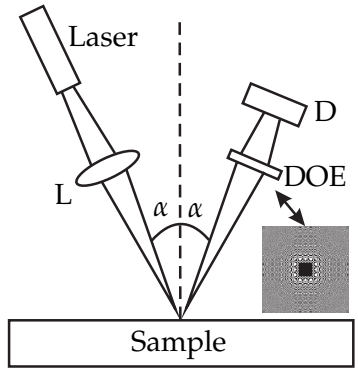

Figure 3.3: Schematic diagram of the handheld wireless glossmeter, L = focusing lens, DOE = diffractive optical element, D = detector (single cell photodiode), α = incident angle. The aperture of the DOE is showed in the inset.

One measurement of the HWDOG consists of 1000 measurement points which are a sequential with time. The measurement time is about 5 seconds, which also includes data transfer to the computer. The measurement data are transferred with the aid of a wireless transmitter to the computer. The result is a gloss profile which permits the calculation of statistical gloss parameters.

In general, conventional glossmeters are calibrated before each measurement series. The new glossmeters presented here do not need calibration before each measurement series because the black glass gloss value is programmed within the measurement software. However, frequently controlling the gloss reference value is desir-

able. Recalibration has to be done if there are changes in the laser intensity level or components of the glossmeter are changed.

3.3 GLOSS MEASUREMENT FROM COLD-ROLLED STAINLESS STEEL PLATES

The purpose of this **Paper I** was to present new solutions for surface gloss inspection for laboratory conditions as well as an application regarding rapid gloss measurement. The measurements were performed for three stainless steel plates, which were cold-rolled. Samples were measured with the HWDOG and the μDOG 2D. Sample A was cold-rolled, heat-treated, pickled, and skin passed. Sample B was dry-brushed and sample C was ground. According to manufacturing of stainless steel plate the average surface roughness (R_a) of the samples varies between 0.2 and 0.5 μm. The first measurement series with the HWDOG contained three different measurements: fixed position, manual scanning in the machine direction (longitudinal direction of the metal plate) and machine cross direction (perpendicular direction to the machine direction). All measurements were repeated five times and the calculated gloss readings and gloss profiles are the average of the five measurements. The lag length was approximately 2 cm and the measurement time for one measurement was approximately 5 s. The speed of scanning varies due to the hand scanning. Fig. 3.4(a) presents three gloss profiles measured at the fixed position with different plates. Fig. 3.4(b) shows three gloss profiles measured by manual scanning in the machine direction, and Fig. 3.4(c) details three gloss profiles measured to the machine cross direction. Part of the gloss variation in Figs. 3.4(b) and (c) is due to manual scanning and another is due to the finishing marks and surface roughness of the samples. Manual scanning was performed by free hand which is a problem because scanning speed is not constant. At the beginning of the gloss profiles in Figs. 3.4(b) and (c) there is a relatively high gloss variation which almost diminishes at the end of the gloss profile. Probably, at the beginning scanning speed is faster and noncon-

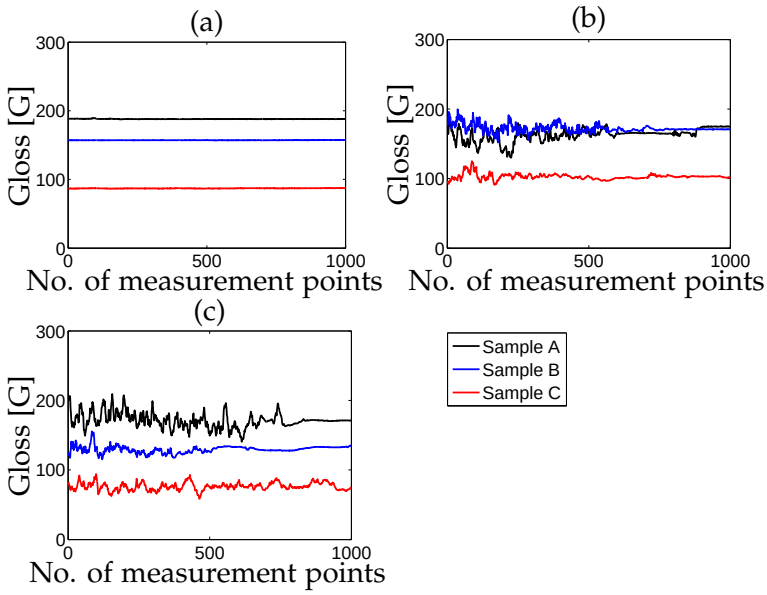

Figure 3.4: Gloss profiles in stainless steel plates measured with the HWDOG. (a) measured in a fixed position (b) measured in the machine direction and (c) measured in the machine cross direction.

stant and at the end of gloss profile scanning speed is almost constant or glossmeter is at fixed position. Therefore, the measurement of the repeatability of the hand scanning is problematic. Also, it is almost impossible to know the exact positions where the measurement starts and ends. There is time-delay before the measurement starts thus exact measurement starting time is difficult to know. To reduce the effect of manual scanning the number of measurements had to be increased.

After the HWDOG measurements, samples were measured with μDOG 2D. The measurement area was 10 mm $\times$ 10 mm and the distance between the adjacent measurement points was 30 μm in both x- and y-direction which correspond to the machine- and machine cross directions, respectively. Therefore, one gloss map consist of ca. 110 000 measurement points. The measurement area was approximately the same as the measurement area when the HWDOG

was used. Fig. 3.5 shows three gloss maps obtained from the stainless steel plates. In the gloss maps in Figs. 3.5(b) and (c) it is possible to observe finishing marks of the stainless steel plates.

The results of the μDOG 2D and HWDOG were compared together and the calculated correlation coefficient (r^2) was 0.84 in the fixed position and 0.95 in the machine cross direction. When the scanning direction of the HWDOG was the machine direction, there was no significant correlation between the μDOG 2D and HWDOG measurement results due to the orientation of the finishing marks because in sample A there are no finishing marks in view as it can be observed in Fig. 3.5(a) therefore the gloss reading in both manual scanning directions were almost the same as it can observe in Fig. 3.6 where is shown the correlation between the μDOG 2D and HWDOG. If the gloss readings in Fig. 3.6 are considered more closely, it can observed that in the sample B and the sample C gloss readings are higher in the machine direction measured with the HWDOG. The gloss reading of these samples depends on the scanning direction and orientation of finishing marks. The same phenomena was shown earlier for the conventional glossmeter in Ref. [6] where it has been shown that gloss readings in the machine direction are higher than the machine cross direction.

However, the results are not statistically significant because the HWDOG measurement series consists only of 5000 measurement

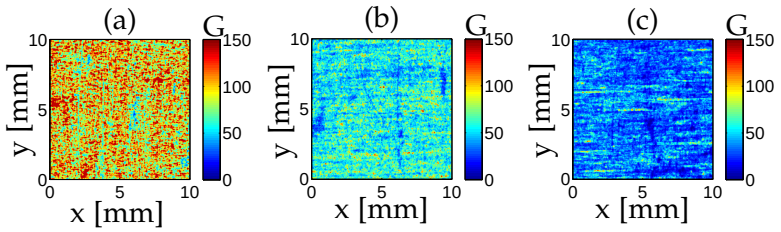

Figure 3.5: Three gloss maps (a) cold rolled (sample A) (b) dry-brushed (sample B) and (c) ground (sample C) measured with the µDOG 2D. The scale of the gloss reading is shown in the colorbar.

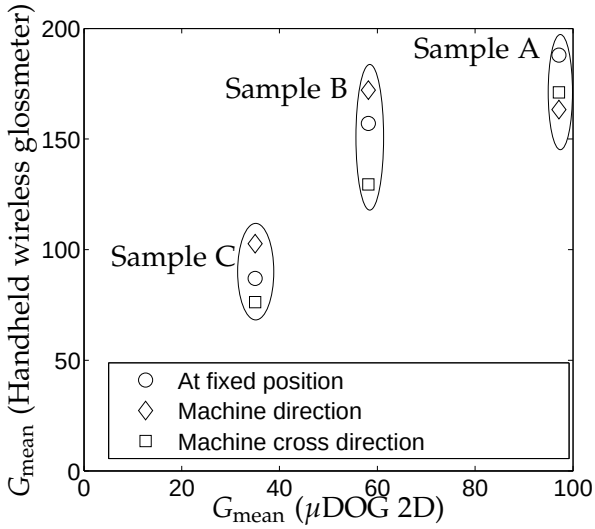

Figure 3.6: Correlation between μDOG 2D and the HWDOG.

points whereas the μDOG measurement consists of over 100 000 measurement points. Therefore, if the better statistical significance is needed the number of measurement of the HWDOG has to increase.

In Fig. 3.6 gloss readings measured with HWDOG are in most cases over 100 G. Also, the part of gloss readings in Fig. 3.5 exceed 100 G. According to definition of the gloss, the polished black glass (gloss reference) gloss reading is exactly 100 GU when the refractive index of gloss reference is equal to 1.567. However, the maximum gloss reading is not defined in the international standard therefore if the refractive index of the sample is greater than 1.567 gloss readings can exceed 100 GU. For example, some metals have very high gloss readings up to 2000 GU [69].

We can observe from Figs. 3.4 and 3.6 that the gloss readings of the HWDOG are higher than those of the μDOG 2D. There are several reasons for this. First, the measurement geometries of these glossmeters are different. In the μDOG 2D the incident angle was 0° whereas in the HWDOG it was 6°. The difference between the incident angles is small but significant because the sample surfaces

were quite glossy. The second reason for the different readings is that the HWDOG scans only a thin line whereas the μDOG 2D scans a macroscopic area; therefore, the number of the measurement points in the case of the HWDOG is less than 5 % of the μDOG 2D measurements points. Dissimilarities between the laser beams shapes and the differences in distance between the samples and glossmeter also influence the different gloss readings.

3.4 ON-LINE PRINT GLOSS MEASUREMENT

In general, regardless of the object, on-line measurements are usually an effective way of reducing production costs because they provide a means of changing production parameters during the process if abnormalities are found, thus reducing the number of the poor quality products [1]. So far, only a few studies have been published on on-line gloss measurements for metal and paper inspection [114, 115].

In this section, a laboratory test series of the μDOG 1D and the results related to the printing line measurements are presented. The series were performed before the installation of the glossmeter on the printing line. They contain a comparison of the conventional glossmeter and the original laboratory DOG, dependence of the measurement signal on the measurement angle of the test surface of a sample and dependence of the gloss readings on the measurement distance between the sample and test surface. After the laboratory tests, the μDOG 1D was installed in the printing line. The measurement series of the printing line contains different measurements performed on the four color heatset web offset printing (HSWO) machine [67] situated at the Forest Pilot Center Ltd. (FPC), Raisio, Finland. More detailed results of the laboratory and printing line test have been introduced in **Paper II**.

The quality of print depends on many things and substantial research has been done for the quality inspection of print and especially using gloss for the estimation of print quality. For example, the paper surface roughness effects on the print [63, 116], surface

topography effects on gloss variation [64], coatings roughness influence [117, 118], the quality inspection of printed matte-coated paper [65], print mottling effects on print quality [27, 119] and ink setting time relation to the print gloss [120]. Print quality depends also on the quality of a printing paper and research has been done for the estimating of the gloss of a coated paper [121–125]. The problem of the previously mentioned studies is that they were performed for the final product. However, gloss of the print products change as a function of time [126]. Therefore, we don't know exactly how changes in different parameters of the printing machine affect on the gloss. The on-line print gloss measurement is one solution because the results can be evaluated immediately therefore it gives a lot of new possibilities to research how different parameters affect on the print quality.

3.4.1 Printing

Printing is a production process where ink is applied to a printing substrate in order to transmit information. Different printing technologies are divided into two categories: conventional printing with a printing plate, such as lithography, and gravure and nonimpact printing, such as electrophotography and ink jet [67].

The on-line gloss measurements in **Paper II** were made at the HSWO printing machine, which is a common indirect printing technology. In HSWO printing, an oil-based paste-like ink is first transferred from the printing plate. The non-image areas of the printing plate are kept ink-free by using a water-based fountain solution. The printing plate transfers the ink film and fountain solution onto a rubber printing blanket cylinder, which applies it to the paper surface. The ink is completely dried in a hot-air oven. More detailed information about HSWO printing and the other printing techniques can be found in [67].

3.4.2 Laboratory tests

The schematic diagram and properties of the μDOG 1D was presented in Fig. 3.2 and section 3.1.2, respectively. At first we made a test series where we compared the μDOG 1D gloss readings with the DOG and the conventional glossmeter. The samples consist of two series which have a different gloss level. Series 1 included 5 glossy samples, and series 2 contained 5 matt samples. Both series included black, cyan, magenta, yellow and unprinted samples. The measurement area of the μDOG 1D and the DOG was 4 mm $\times$ 4 mm and in the conventional glossmeter measurement the area was an ellipse with axel lengths of 7 mm and 13 mm, respectively. The calculated beam width of the DOG was 40 μm at $1/e$-level and the distance between the adjacent measurement point in both directions was 40 μm. With the μDOG 1D the distance between the adjacent measurement lines was 40 μm for the linear scan using the x-y-z-translation stage. Therefore, the measurement of the DOG and μDOG 1D consisted of 10 000 and ca. 50 000 measurement points, respectively. The gloss measurement of the conventional glossmeter consists of ten measurements. Five measurements were performed in the machine direction, i.e. the longitudinal direction to the paper web, and the other five measurements were made in a machine cross direction, i.e. perpendicular to the machine direction. The location of the measurement area of the conventional glossmeter was approximately the same as the measurements of DOG and μDOG 1D. However, due to the measurement geometry, and differences in optics the illuminated area of the conventional glossmeter was larger. The measurements results are shown in Fig. 3.7. The calculated correlation coefficient between the DOG and μDOG 1D was r^2 = 0.96 for the mean gloss G_{mean} and r^2 = 0.97 for the gloss variation G_{a}. The correlation between the μDOG 1D and the conventional glossmeter was r^2 = 0.84. The lower correlation between the μDOG 1D and the conventional glossmeter is due to the fact that the measurement geometry 60° used for the conventional glossmeter is too low for the part of the matt sample series. Measurements of the 75°

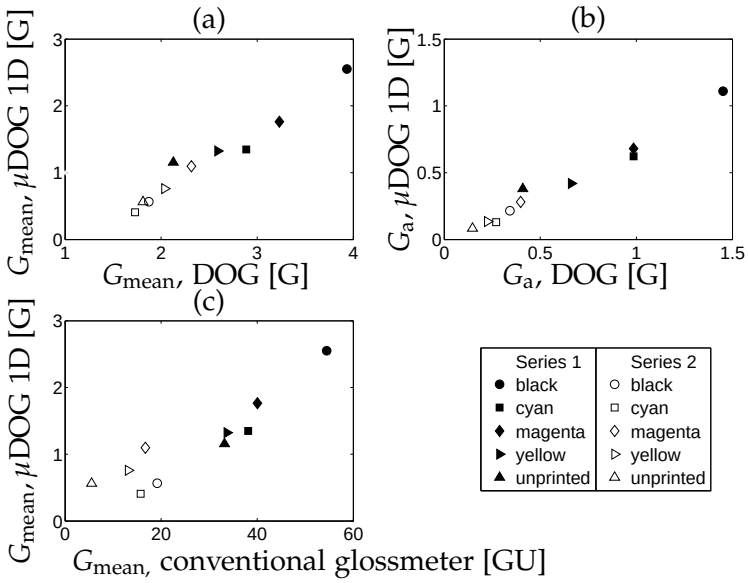

*Figure 3.7: (a) Mean gloss G_{mean} (b) gloss variation G_a measured with the DOG and μDOG 1D and (c) mean gloss measured with the conventional glossmeter and μDOG 1D (See Fig. 2 of **Paper II**).*

geometry would give better results for the matt sample series. Also differences between the measurement geometries and light sources have an effect on gloss readings. In Ref. [5] has been shown the diagram which describes how gloss readings and visual appearance behave with different gloss measuring geometries. The diagram is approximation but it shows that gloss readings below 20 GU are better to measure with higher angle of incidence. The measurement error of the μDOG 1D in the average gloss value G_{mean} is smaller than 0.02 G and the error in the average gloss variation G_{a} is approximately 1 % of the G_{mean} value. The error in the G_{a} value occurs partly from the fluctuations of the laser intensity. Approximations of errors have been measured in the laboratory thus they can be different in the printing house environment, because in the printing house environment there are many potential error sources such as external light and vibration of the printing machine which

can be eliminated in laboratory.

In the printing machine the paper web can fluctuate slightly in the vertical direction. Therefore, we had to determine how large an effect the paper web movement has on the gloss reading. Gloss readings were measured as a function of the distance between the sample and the μDOG 1D. The sample and the measurement technique were the same as previously presented in the correlation measurement. The same area was scanned using five different distances between the glossmeter and the sample. The measurement distance was changed over the range 105 mm-109 mm at intervals of 1 mm. The focal length of the laser beam was earlier defined at a distance corresponding to the 107 mm distance between the sample and the glossmeter. The results are shown in Fig. 3.8. The mean gloss G_{mean} increases and gloss variation G_{a} varies slightly when the distance

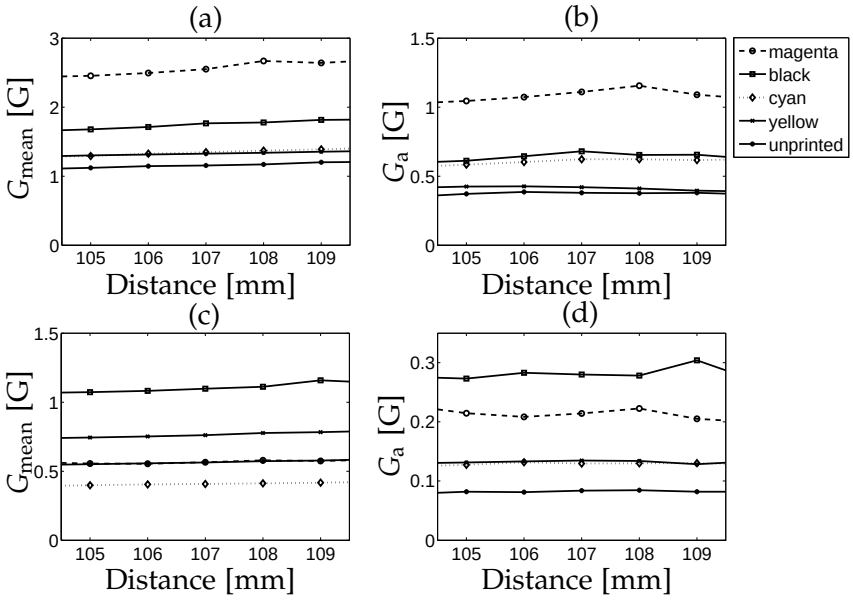

Figure 3.8: Mean gloss G_{mean} and the gloss variation G_a as a function of measurement distance. (a) G_{mean} values and (b) G_a values of series 1. (c) G_{mean} values and (d) G_a values of series 2. The measurement distance 107 mm correspond to the focal length distance (See Fig. 3 of ***Paper II****).*

between the glossmeter and sample decreases. The reason for the increasing G_{mean} values is that more light propagates through the aperture of the DOE when the distance between the sample and glossmeter decreases. The result shows that small fluctuations of gloss readings as a function of the distance between the sample and glossmeter are tolerable, thus it has not significant effect on on-line gloss measurement. The third test measured the dependence of the measured signal on the angle of the surface of a sample. The purpose of this test was to simulate the angular displacement of the paper on the printing machine. The test was performed with polished black glass (gloss reference) fastened to the electrically driven flatbed rotator. The measurement were performed at the range of -1° to 1° with a 0.1° steps. The results in Fig. 3.9 show that measurement results depend on the tilt angle. The maximum gloss reading is obtained at the 0° angle (i.e. incoming light beam and gloss reference are perpendicular) and the maximum gloss value

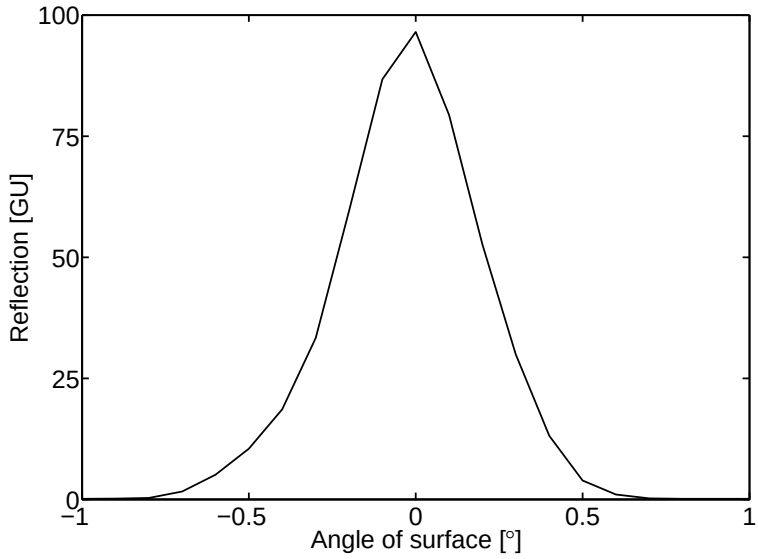

Figure 3.9: Reflection as a function of tilt angle obtained from the polished black glass (See Fig.3 of ***Paper II****).*

is slightly less than 100 G. According to Eq. 3.2 the gloss reading for the black glass is exactly 100 G. The difference between the measurement result and the definition of the gloss is due to the fact that the polished black glasses are not uniform [36,79]. If the tilt angle is $\pm 1^{\circ}$ the gloss reading is zero thus reflected light is not going to detector. In the real printing samples, The shape of the curve for prints is similar to that of the gloss standard except the difference between the highest and the lowest gloss value is smaller. Therefore, the angle between the incoming light and paper web of the printing machine has to be check before each measurement.

3.4.3 Measurements at the printing line

After the laboratory test series, the on-line glossmeter was installed in the printing line. The glossmeter was installed after the hot air dryer of the printing machine close to the draw cylinder which minimized the vertical movement of the paper web.

The analysis of the μDOG 1D measurement data is based on the gloss profile arrangement for the gloss matrix using a fast Fourier transform (FFT). Fig. 3.10(a) presents the arranged gloss matrix where five different patches of printed sheet are shown. The patches are, from top to bottom, black (B), unprinted (U), yellow (Y), cyan (C) and magenta (M). In Fig. 3.10(a), the vertical direction indicates the number of measurement points and the horizontal direction the number of printed sheets. 3.10(b) presents the mean, maximum and minimum gloss readings of the arranged gloss matrix in the direction of the printed sheets. The calculated statistical gloss parameters G_{mean} and G_{a} with the different patches and all the data of the trial point are presented in Table 3.1. Statistical gloss parameters in Table 3.1 show that magenta and yellow have the highest gloss readings, which is obviously because magenta and yellow reflect well red light. The result is consistent with the previous study with the original DOG [33]. More results on the on-line measurements can be found in **Paper II**.

The speed variations of the paper web cause problems in the

arrangement of the gloss matrix because the number of sampling points of one printed sheet decrease when the speed increases and when the speed decreases the number of the sampling points increase.

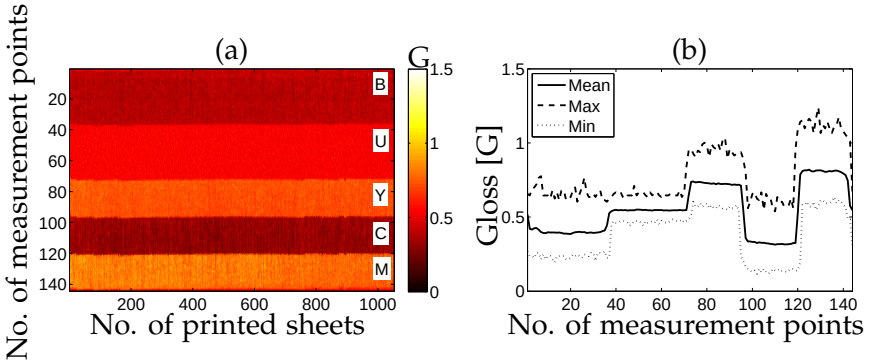

Figure 3.10: (a) Arranged gloss matrix from the gloss profile of the trial point. The scale of gloss reading G is shown in the sidebar. From the top of the matrix to the bottom, gloss readings are measured from black (B), unprinted (U), yellow (Y), cyan (C) and magenta (M) patches. (b) Mean, maximum and minimum lateral profiles of arranged gloss matrix in the direction of printed sheets.

Table 3.1: Calculated statistical gloss parameters, mean gloss G_{mean} and the gloss variation G_a of the full trial point and the different part of trial point presented in Fig. 3.10.

Part of trial point	$G_{\mathrm{mean}}[G]$	$G_{\mathrm{a}}[G]$
Full	0.54	0.15
Black	0.40	0.05
Unprinted	0.55	0.02
Yellow	0.73	0.04
Cyan	0.32	0.05
Magenta	0.81	0.06

3.5 SENSOR FOR GLOSS AND SURFACE ROUGHNESS MEASUREMENT

The measurements of gloss and surface roughness have been made separately with different gauges as in Ref. [28]. This is due to the fact that there has thus far been no single gauge which is able to measure both gloss and surface roughness.

Next a novel single sensor for both gloss and surface roughness measurement is presented by a combination of two optical measurement setups. The schematic diagram of the setup is presented in Fig. 3.11 and is quite similar to that of the original DOG represented in Fig. 3.1. The detectors in this study were CMOS cameras, the signal of the gloss measurement was recorded with the CMOS 1, and the signal of the surface roughness measurement was recorded with the CMOS 2. The principle of gloss measurement is the same

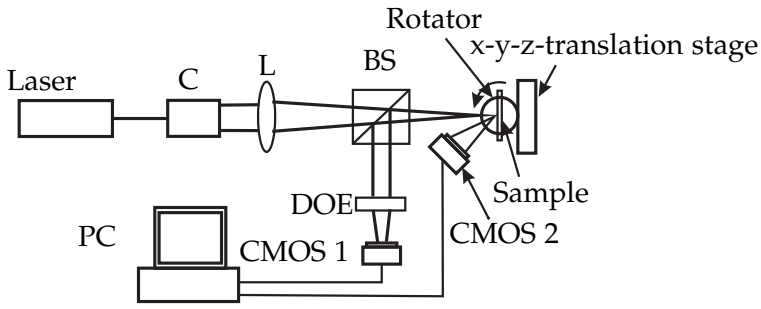

Figure 3.11: Schematic diagram of gloss and surface roughness measurement setup. L = Lens, C = collimating optics, BS = Beam splitter, PC = Personal computer, DOE = Diffractive optical element, CMOS 1 = CMOS camera in the gloss measurement direction, CMOS 2 = CMOS camera in the surface roughness measurement direction.

as presented in section 3.1. The surface roughness measurement is based on the angular speckle correlation measurement with two different speckle patterns [94–97,100,101]. Both the rotation stage and the *x*-*y*-*z*-translation stage are computer-controlled. The calculated focus size was 20 μm at the $1/e$-level of the maximum of irradiance of the beam. The illumination angle of the laser beam was 0° for the detection of gloss. The sample was scanned with the aid of a *x*-*y*-*z*-

translation stage, and thus the image was recorded after each step of the scanning. The result is a gloss map consisting of individual calculated gloss readings. The surface roughness was measured in the following way: the first speckle pattern was recorded at normal incidence and the second pattern at the same point after the sample was rotated. The rotation angle was 0.6°. The sample was scanned similarly to the gloss map and the result is a correlation map which consists of individual C parameter values.

3.5.1 Results

We measured three samples of the metal surface roughness standards (produced by Flexbar Machine Corporation). The samples were machined by grinding. The average surface roughnesses R_a of these samples were 0.4, 0.8, and 1.6 μm. The measurement area was 1.5 mm $\times$ 1.5 mm and the distance between the adjacent measurement points was 20 μm. Therefore the measurement area consists of ca. 5500 measurement points. In Fig. 3.12 shows measurement data calculated by using Eqs. 2.9, 2.2 and 3.2. In Fig 3.12(a), the parameter C is presented as a function of the average surface roughness R_a. In Fig 3.12(b), the mean gloss (G_{mean}) is presented as a function of the parameter C, and in Fig 3.12(c) the mean gloss is presented as a function of the average surface roughness. The calculated correlation coefficients (r) were -0.98, 0.98 and -0.98, respectively. It has previously been shown that since angular speckle correlation and average surface roughness have a negative correlation [96], and mean gloss and average surface roughness also have a negative correlation [6], the results are feasible. Even though the results are relatively good, we have to remember that the measurements were done only for the three samples with surfaces that were quite homogenous; thus the calculated correlation coefficients are only the reference and are not statistically significant. With the aid of Eq. 2.10 it is possible to calculate the surface roughness value corresponding to the C parameter. However, Eq. 2.10 proposes that the surface must follow Gaussian statistics, which is not the case for

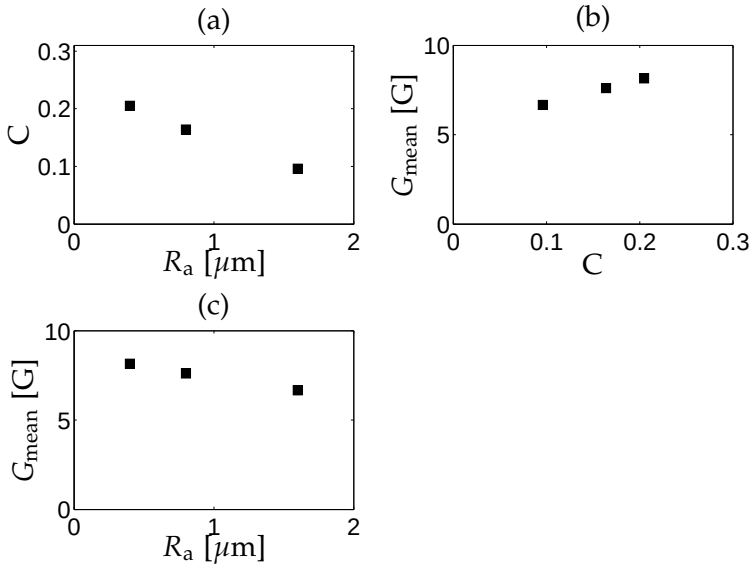

Figure 3.12: (a) The correlation as a function of average surface roughness (R_a). (b) Mean gloss (G_{mean}) as a function of correlation and (c) mean gloss (G_{mean}) as a function of average surface roughness (R_a).

the surface finish of the present samples. Hence, *C* parameter is suggested as the measure for surface roughness. This aids in the optical inspection of surfaces to arrange the surfaces in the correct order concerning surface roughness. Fig. 3.13(a), presents a gloss map of the sample with R_a = 1.6 μm and Fig. 3.13(b) demonstrates the corresponding *C* parameter map of the same area to the gloss map in 3.13(a). If we consider Fig. 3.13(a), there are areas which are glossier (brighter areas) than the surrounding area. If the same areas are considered in Fig 3.13(b), it can be noted that the *C* parameter is high and close to 1. This means that the measurement technique for gloss and surface roughness measurement are consistent.

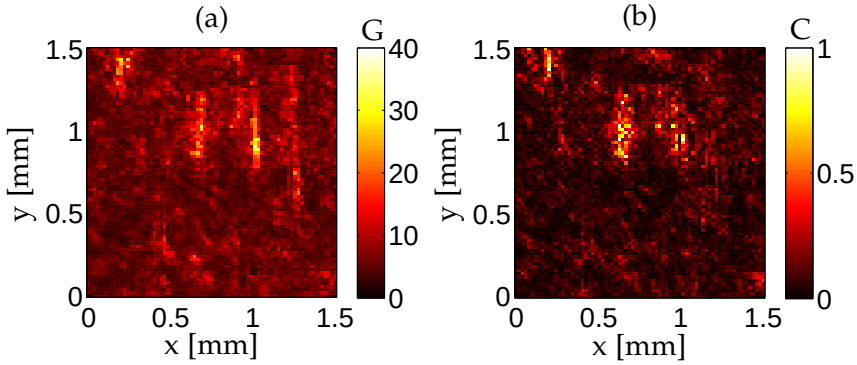

Figure 3.13: (a) Gloss map, and (b) the C parameter map obtained from a metal surface roughness standard with average surface roughness R_a=1.6 µm.

3.6 DISCUSSION

The main focus of this chapter was the development of the original DOG and three prototypes of the new generation DOGs which have been developed for different purposes. The experimental part of this chapter considered different measurements of the DOGs regarding cold-rolled stainless steel products and on-line measurement of gloss at the printing house. In addition, a single sensor which is able to measure both the gloss and the surface roughness was presented.

The cold-rolled stainless steel plates were measured with the HWDOG and μDOG 2D. One purpose of this study was to determine whether the HWDOG is an inexpensive and practical tool for the gloss inspection of products in the metal industry since it gives not only a numerical gloss reading on its display but also a gloss profile from which statistical gloss parameters can be calculated. The HWDOG is wireless, thus it offers new possibilities for product inspection. The second glossmeter used in this study was the μDOG 2D, which gives comprehensive data about the measured stainless steel plates. The measurement result of the μDOG 2D is a gloss map which is a visual presentation of the gloss variations of the scanned surface. Using the gloss map we can find locations

where the gloss is abnormal. Furthermore, the statistical gloss parameters can be calculated for the measurement data. Because the measurements of the HWDOG were performed by free hand there are limitations which one has to take into account regarding the repeatability of the measurement.

The third glossmeter application considered in this chapter was the μDOG 1D which was designed for on-line measurement in the printing line. The laboratory test series and measurements at the printing line show that the μDOG 1D is capable of on-line gloss measurement in the printing line of a heatset web offset printing machine. The results show that the gloss profile can be measured as a function of measurement time, and the measured gloss profile can be presented as an arranged gloss matrix. Statistical gloss parameters can be calculated for the full gloss profile, a particular trial point or the particular patches of the arranged gloss matrix as shown in Table 3.1. The μDOG 1D is also capable of detecting small gloss variations. The presented on-line glossmeter could be useful in other fields of industry such as metal, paper, and laminated materials.

The third part of the experimental work in this chapter consisted of a method for gloss and surface roughness measurement using only a single setup. The measurements were performed for three metal surface roughness standards which were machined by grinding. The measurement results show that the method works for these particular samples. It is obvious that simultaneous information on the gloss map and surface roughness via the correlation map provides more rigorous information on the surface quality than the gloss or surface roughness readings alone. Both the gloss and the correlation map give microscopic and macroscopic information about the measured sample area. This has an advantage over traditional measurement devices. Another advantage of this method is that gloss and surface roughness are both measured exactly at the same location, which would be almost impossible to carry out if they were measured separately with different gauges. We expect that it will also be possible to use this measurement method and

sensor for the measurement of gloss and surface roughness from a porous surface, such as, a pharmaceutical tablet.

The presented measurement method for the gloss and surface roughness measurement is not yet complete for on-line measurement because the recording and analysis time of the two speckle patterns is relatively long. Another factor limiting the use of this method for the on-line inspection of gloss and surface roughness of objects is the need to record two speckle patterns with different illumination angles, which is difficult to implement.

The advantage of all the DOGs presented is that only one measurement geometry is needed, i.e. the surface normal (except HW-DOG, where the angle of incidence is 6°) direction, where the effect of polarization is small. DOGs also have better sensitivity than conventional glossmeters because of the small spot size and since the measurement data of the DOG consist of more comprehensive data.

4 Development of diffractive element based glossmeters for curved object inspection

The measurement of the gloss of a curved surface is quite problematic because the international standards for gloss measurement [10,11] have only been defined for a flat surface. There are only few glossmeters which are valid for a curved surface [69–71], and are used for agricultural products inspection. Nevertheless, there are some limitations on these glossmeters, such as their having been development only for laboratory use and a relatively large surface, which is problem when the curvature of the radius of an object is small. In this chapter, we present two DOGs which can be used in gloss measurements of both convex and concave surfaces. The DOGs for the curved surface were modified from the original DOG and the HWDOG (see chapter 3). The gloss measurement of convex and concave surfaces is performed for unpainted and painted aluminium samples. In addition, we present an application for using a modified DOG where a latent fingerprint is recorded from a ballpoint pen. This application has important implications in forensic studies. The gloss measurements of the curved surface are presented in **Papers III** and **IV**.

4.1 DOGS FOR A CURVED SURFACE

The schematic diagram of a DOG for a curved surface is shown in 4.1. In the original DOG, the sample can be scanned in the x- and y-directions whereas the DOG for the curved surface sample is scanned for the vertical direction (y-direction) and rotated after every measured column. The construction of the optics HWDOG for

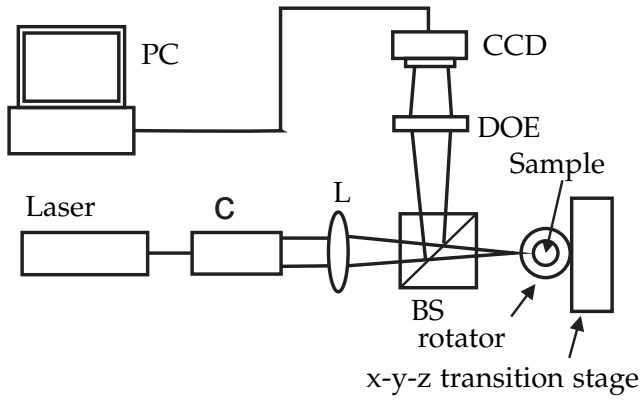

Figure 4.1: Schematic diagram of the DOG for a curved surface. BS = beam splitter, C = collimating optics, L = focusing lens, DOE = diffractive optical element, CCD = charge-coupled device, PC = personal computer.

the curved surface is the same as the HWDOG represented in Fig. 3.3. The commercial flat jig is replaced according to the idea of the author of this thesis by jigs with convex and concave shapes which fit the cylinder shapes studied of the samples. The purpose of the jigs is that in manual scanning we try to keep the angle between the glossmeter and the sample the same for each measurement, which guarantees better repeatability.

4.2 EXPERIMENTAL

4.2.1 Gloss measurement of convex and concave aluminium samples

Both sample series, convex and concave consist of unpainted, black painted and white painted aluminium samples. The painted samples were painted with matte spray paint. The samples were measured with both DOGs. Fig. 4.2 shows the measurement directions of the convex and concave samples.

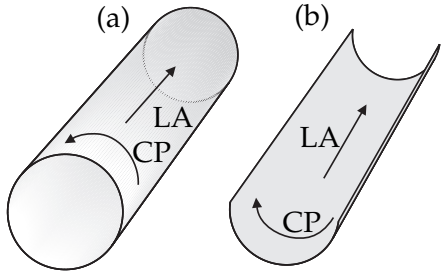

*Figure 4.2: The measurement directions for (a) convex and (b) concave samples. LA = longitudinal axis and CP = circular path (See Fig.3 of **Paper III**).*

At first, samples were measured with the DOG. The measurement area of the DOG measurement was 10 mm in the longitudinal direction (LA) and 40 mm for the circular path (CP). The distance between the adjacent measurement points was 30 μm in both directions. The measured gloss maps of the DOG for the convex and concave samples are presented in Fig. 4.3. On the left-hand side are the measured gloss maps for the concave series and on the right-hand side are the measured gloss maps for the convex sample series. In Table 4.1 is presented calculated gloss readings, average gloss G_{ave} and gloss variations G_{var}. The gloss readings were calculated with the aid of Eqs. 2.5 and 2.6.

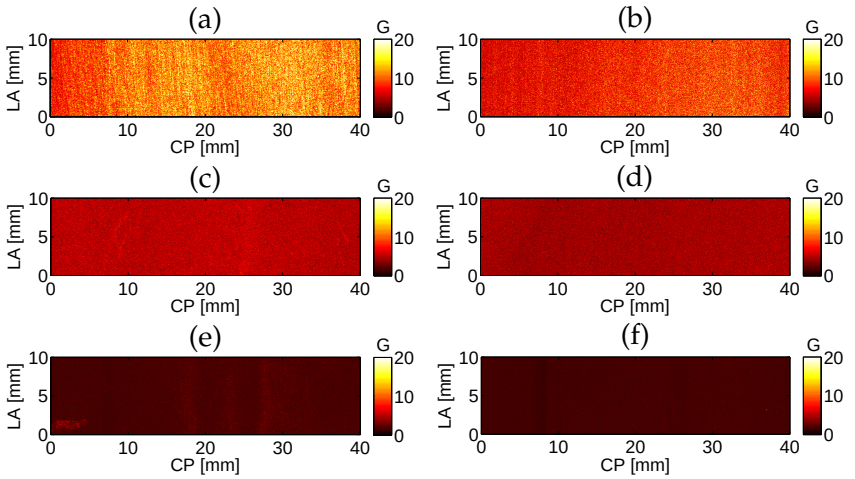

*Figure 4.3: Measured gloss maps from the convex and the concave sample series obtained with the DOG: (a) concave aluminium, (b) convex aluminium, (c) concave white painted, (d) convex white painted, (e) concave black painted, (f) convex black painted (See Fig. 4 of **Paper III**).*

The samples were also measured with the HWDOG. Each sample was measured 10 times along a circular path and longitudinal axis. The measurement results are the gloss profiles presented in Fig. 4.4. The statistical gloss parameters were calculated from the gloss profiles with the aid of Eqs. 2.5 and 2.6 and they presented in the Table 4.2. The gloss profiles and statistical gloss parameters are the average of ten manual scans. The lag length of the scans was approximately 2 cm. The exact lag length of the HWDOG is impossible to find out because it is difficult to define exact starting and ending point. This and the other measurement problems of the HWDOG were considered in the case of the flat surface in section 3.3, and they are also valid in the case of a curved surface. From Figs. 4.3 and 4.4 and Tables 4.1 and 4.2 indicate that the unpainted samples have the highest gloss independent of the measurement

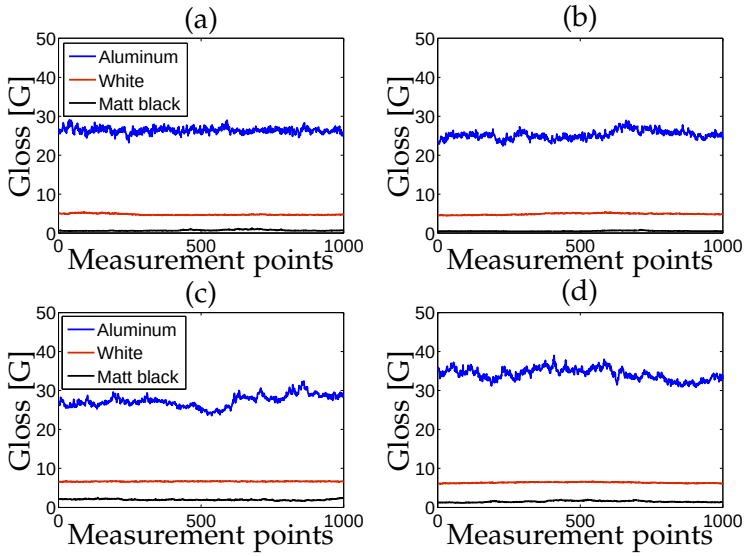

Figure 4.4: Measured gloss profiles of the convex aluminium samples along (a) the longitudinal axis and (b) the circular axis, and for the concave aluminum samples along (c) the longitudinal axis and (d) the circular axis.

directions and the white painted samples are glossier than those painted black. The results of the DOG and the HWDOG support the visual inspection, which was made before the measurement series. For the unpainted aluminium samples, the HWDOG gives a much higher gloss reading than the DOG. There is no individual reason for this, because several individual things have an effect on high gloss reading. The incident angle of the HWDOG is larger. The difference in the incident angles is only 6° but this is significant when the sample is glossy, and we measured the irradiance of the specularly reflected light. The DOG is a noncontact glossmeter, whereas the HWDOG is a contact glossmeter. Therefore, the geometries of these two glossmeters are different and hence the distance between the DOE and the sample is different. In addition the size of the apertures and the focal lengths of the DOE are different. In the HWDOG, the aperture size is 2 mm $\times$ 2 mm and the focal length is 20 mm whereas in the DOG its aperture size is 4 mm $\times$ 4

mm and the focal length is 100 mm. Moreover, light sources and detectors between the two glossmeters are different. The light source in HWDOG was a semiconductor laser and the detector was a photodiode whereas in DOG they were HeNe laser and CCD-camera, respectively. Therefore the shapes of laser beams and sensitivity of the detectors are different.

The gloss maps in Fig. 4.3 and the gloss variation reading in Tables 4.1 and 4.2 show that the samples were not uniform. In other words, there are gloss variations resulting from the quality variations of paint in the painted samples and surface irregularities in the aluminium samples i.e. surface roughness. The results of Figs. 4.3 and 4.4 show that both glossmeters are able to detect quite low gloss readings, as in this case of black painted samples.

We calculated correlation between the DOG and the HWDOG for circular path measurements.For the concave series it was $r^2 = 0.95$ and for the convex series it was $r^2 = 0.92$. Even if these results were good, they were not statistically significant because lack of the measurement points of HWDOG the measurement of the HWDOG consists of 10 000 measurement points and that of the DOG consists of approximately 450 000 measurement points. If we want to increase statistical significance, the number of measurement points has to increase. However the main idea of this study was the same as in section 3.3 and **Paper I**. We have two glossmeters, at first, the HWDOG can be used for the quick gloss inspection. If there are abnormalities the sample is possible to measure with the DOG which gives a more comprehensive gloss map.

In Table 4.2 we can observe that gloss readings for the concave series are higher than in convex series which result from the fact that the radius of curvature of these series is different thus convex and concave series are different. Therefore it is difficult to compare these two series.

Table 4.1: Measured average gloss G_{ave} and gloss variation G_{var} for the convex and concave samples obtained with the DOG.

Sample	G_{ave} [G]	G_{var} [G]
Convex		
Aluminium	8.33	2.13
White	4.67	0.83
Black	1.91	0.18
Concave		
Aluminium	11.33	2.60
White	5.37	0.76
Black	2.08	0.25

Table 4.2: Measured average gloss G_{ave} and gloss variation G_{var} for the convex and concave samples obtained with the HWDOG along longitudinal axis and circular axis.

Sample	Longitudinal axis		Circular Path	
	G_{ave} [G]	G_{var} [G]	G_{ave} [G]	G_{var} [G]
Convex				
Aluminium	26.36	1.93	25.23	2.18
White	4.76	0.25	4.87	0.30
Black	0.66	0.25	0.49	0.17
Concave				
Aluminium	27.36	2.19	34.19	3.74
White	6.65	0.15	6.35	0.24
Black	1.97	0.38	1.49	0.45

4.2.2 Latent fingerprint measurement from a convex surface

Fingerprints are one of the most widely used biometric methods for identifying and authenticating individual persons [127]. Fingerprints consist of the friction ridges and valleys, when the finger touches a surface it leaves salt and different organic compounds on the surface [128]. Fingerprints are divided into two different categories: exemplar fingerprints, which are easy to detect bye an eye and latent fingerprints which are partially hidden and therefore difficult to detect. A traditional way of recording fingerprints on a surface is the applied powder lift of the fingerprint with a tape where the fingerprint is photographed. However, the problem with this method is that the fingerprint can be destroyed when it is recorded on the surface. Therefore the number of different optical methods and imaging techniques have been developed because they provide the non-destructive measurement of fingerprints on a surface. These techniques are, for example, based on the light detection of the reflected polarized light [127], optical coherence tomography (OCT) [128–130], Raman chemical imaging [131] and the biometric method that combines the finger-vein, fingerprint and finger geometry features [132].

The problem with the previously mentioned methods is that they work only for a flat surface. The DOG can be used for detecting a fingerprint non-destructively from a smooth and curved surface. This technique is based on the detection of gloss variation (Ref. [24] and **Paper III**) between the friction ridges and valleys. The measurement setup was presented in Fig. 4.1. The rotator in this study was a motor-driven rotary stage. In this study, the calculated spot size of laser beam was 10 μm.

Fig. 4.5(a) shows a photo of the ballpoint pen and Fig. 4.5(b) shows the glossmap recorded from the pen. The fingerprint in Fig. 4.5(b) is detected in the middle part of the ballpoint pen near the gold horizontal stripe (red square). This stripe is on the bottom of the gloss map where the stripe is in red. The red color in Fig. 4.5(b) indicates a high gloss and blue color indicates low gloss ar-

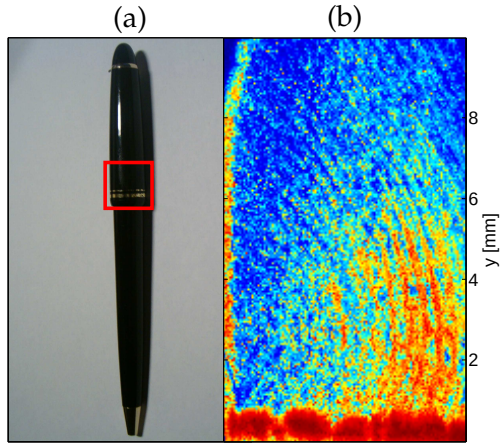

Figure 4.5: (a) Ballpoint pen. The latent fingerprint located in the middle section of the pen near the gold horizontal stripe. Red square indicates the measurement area. (b) latent fingerprint detected from the ballpoint pen.

eas. The advantage of this method is that it works both to curved and flat surfaces and the sensitivity of DOG is good because it can detect small gloss variations. This technique was tested for a surface which is quite smooth. Before this technique can be used real crime scene investigation it has to be tested with other surfaces, such as rough and porous surfaces. The comparison to the other fingerprint detection methods is needed to find out real potential for the use this technique. Because the lack of techniques for the curved surface, the comparison between the other fingerprint detection methods can be performed at first for flat surfaces with the original DOG and the μDOG 2D. If the results were satisfactory, there will be a real potential for using this method also for curved surface inspection.

4.3 DISCUSSION

In this chapter we presented two new optical measurement setups for gloss inspection from a curved surface. In the first setup the DOG was modified from the original DOG (see Fig. 3.1) and in the second the HWDOG was modified from the commercially available glossmeter. Both of these DOGs are useful for measurements in laboratory conditions and the HWDOG also shows potential for quick product inspection in industrial off-line measurements in situations when abnormalities in a sample appear and we need to confirm our visual interpretation. The advantages of the DOGs for curved surface gloss measurement are that they can be used both for convex and concave surfaces. It is also possible to inspect small areas because of the small spot size of the laser beam. The gloss map which can be obtained with the DOG is useful for gloss inspection because it gives many more details about the inspected surface than the pure numerical value of the gloss or gloss profile. Glossmeters used for curved surfaces in Refs. [69–71] give only numerical gloss readings.

The measurements of the curved surface were performed for a cylinder surface which is a special case of a curved surface. However in most cases the shape of the curved surface is not a cylinder. The DOG works other curved surface but it depends a lot of a shape of a surface. Therefore, if the shape of the surface is complicated it is better to limit the measurement area.

In addition, an application for the latent fingerprint measurement of a convex surface was presented in this chapter. The technique is based on the fact that the DOG can detect small gloss variations since fingerprints leave salt and organic compounds on the surface. This application would be useful for crime scene investigation. However, it requires much more research to determine if there is any potential use in this field. There are some limitations of the use of this technique in real situation. Fingerprint measurement on the curved surface requires special knowledge about the DOG. The described method has been tested only for a ball point pen which

shape is not exactly a cylinder but we can approximate it as a cylinder surface. Also the measurement time has to be shorten before this technique is ready to use in crime scene investigation. The fingerprint measurements have been also tested for a flat surface by using the μDOG 2D which was presented in sections 3.2.1. μDOG 2D is straightforward to use but the problem is that there are several good techniques for recording the fingerprint on a flat surface thus there is not necessarily need for the new techniques.

There are several standards for the measurement of gloss on a flat surface [10,11], but none for curved surface gloss measurement; this is quite problematic. For example, calibrating the DOG is problematic because we had to use the same gloss reference we used for the flat surface. It would be quite problematic to generate gloss reference for the curved surface because if the radius of curvature of a sample change we need different gloss references. Because the lack of gloss reference for the curved surface, the results depends on more or less light on the light source, measurement geometry, detector and surrounding environment. However, in most of the cases it is enough that we can compare the differences of gloss readings within the same sample series.

5 Conclusion

The main focus of this thesis was the development of new generations of DOG and the measurement techniques and analysis of the gloss of flat and curved surfaces. The analysis of the gloss is based on the use of statistical gloss parameters which have been earlier defined for a flat surface [24]. The measurement and analysis of gloss are rather straightforward for flat surfaces. However, this is not the case with curved surfaces. Therefore the statistical gloss parameters for the curved surface were presented in chapter 2 and glossmeters for the curved surface in chapter 4.

In chapter 3, the development of the DOG for a flat surface was considered. The original laboratory and the new generations of DOGs were presented. The μDOG 1D was developed for on-line gloss measurement, the μDOG 2D for flat surface inspection in laboratory conditions and the HWDOG for rapid gloss inspection. Measurement with the μDOG 2D and the HWDOG were performed for a cold-rolled stainless steel plate. The results show that the HW-DOG and μDOG 2D work separately. The best results is achieved with the μDOG 2D because it gives a detailed gloss map where the abnormalities of the gloss can be found. However, the optimal results were achieved when the HWDOG and μDOG 2D are used together. The product is first measured quickly with the HWDOG, if there are abnormalities the product can be measured with the μDOG 2D.

The HWDOG could find application in field conditions that may include gloss inspection of gloss decrease of paint of metal pipes or log houses. Especially paint industry is interested in paint wear due to weather conditions, and gloss is one quality factor that is monitored in field experiments of paint wear. If we relax the hand scanning and adjust the small size HWDOG into an arm of a robot. The repeatability of gloss measurement is naturally improved. Then it is possible to arrange non-contact measurement e.g. different

painted and non-painted parts in car industry.

The on-line glossmeter (μDOG 1D) tests in laboratory show that the gloss readings of the μDOG 1D were consistent with the original DOG and the conventional glossmeter. Other test results indicate that the vertical movement of the sample has a negligible effect on the gloss readings and the measurement results depend on the angle between the sample and incoming beam. The on-line measurements in the printing line show that the μDOG 1D is capable of on-line measurement and the results can be presented as a useful gloss profile and an arranged gloss matrix.

In addition, a solution to the problem of simultaneous gloss and surface roughness measurement using a single sensor was presented in chapter 3. The gloss measurement was based on reflected light measurement with the aid of the DOG and the surface roughness measurement was based on an angular speckle correlation measurement. The measurement results show that the method works for these particular samples, which were from the metal surface roughness standard. However, data processing has to be improved because the measurement time is relatively long.

Gloss measurements from convex and concave surfaces are problematic because of the lack of suitable glossmeters. In chapter 4, two solutions for curved surface gloss measurement were presented. The DOG and HWDOG that were used were modified from the original DOG and HWDOG for the flat surface, respectively. The measurements were performed with unpainted and painted convex and concave aluminium samples. The results show that both DOGs can detect gloss variations and low gloss readings. The results of these two DOGs were consistent. In addition, one application of curved surface gloss measurement was presented in chapter 4, where a latent fingerprint was detected from a ballpoint pen. There will be many further possibilities for applications of curved surface gloss measurement because of the lack of proper glossmeters.

The presented measurement techniques do not obey existing gloss standards. However, the advantage of the used method is that we need only one measurement angle which works for both low

gloss and high gloss surface whereas according to different gloss standards there are total in 5 different measurement angles. The used measurement geometry made it possible to inspected gloss of curved surface. Therefore there will be an opportunity to realize a standard for this gloss measurement method. The biggest problem is that people who work in the field of the product quality inspection do not always understand if we have two different gloss readings from the same sample which mean the same but they were measured with different measurement geometry.

Bibliography

[1] P. Cielo, *Optical Techniques for Industrial Inspection* (Academic Press, London, 1988).

[2] M. Landy, "Visual perception: A gloss on surface properties," *Nature* **447,** 158–159 (2007).

[3] H. Assender, V. Bliznyuk, and K. Porfyrakis, "How surface topography relates to materials' properties," *Science* **297,** 973–976 (2002).

[4] W. Ji, M. Pointer, R. Luo, and J. Dakin, "Gloss as an aspect of the measurement of appearance," *J. Opt. Soc. Am. A* **23,** 22–33 (2006).

[5] R. Hunter and R. Harold, *The measurement of appearance* (Wiley-Interscience, New York, 1987).

[6] R. Silvennoinen, K.-E. Peiponen, and K. Myller, *Specular Gloss* (Elsevier, Amsterdam, 2008).

[7] G. Obein, K. Knoblauch, and F. Viénot, "Difference scaling of gloss: Nonlinearity, binocularity, and constancy," *J Vis* **4,** 711–720 (2004).

[8] J. Wills, S. Agarwal, D. Kriegman, and S. Belongie, "Toward a perceptual space for gloss," *ACM T. Graphic.* **28** (2009).

[9] Y.-X. Ho, M. Landy, and L. Maloney, "Conjoint measurement of gloss and surface texture," *Psychol. Sci.* **19,** 196–204 (2008).

[10] "Standard Test Method for Specular Gloss. Designation: D523-89," *American Society for Testing and Materials, West Conshohocken, USA* (1989).

[11] "Paints and varnishes- Determination of specular gloss of non-metallic paint films at 20, 60 and 85 deg. ISO 2813:1994(E)," *International Organization for Standardization, Geneve, Switzerland* (1994).

[12] J. Liu, M. Nöel, and J. Zwinkels, "Design and characterization of a versatile reference instrument for rapid, reproducible specular gloss measurements," *Appl. Opt.* **44,** 4631–4638 (2005).

[13] W. Budde, "A reference instrument for 20°,60° and 85° gloss measurements," *Metrologia* **16,** 1–5 (1980).

[14] G. Andor, "Gonioreflectometer-based gloss standard calibration," *Metrologia* **40,** S97–S100 (2003).

[15] K. Myller, *A glossmeter based on a diffractive optical element*, PhD thesis (University of Joensuu, Joensuu, Finland, 2004).

[16] M. Juuti, *Detection and analysis of local gloss of media*, PhD thesis (University of Joensuu, Joensuu, Finland, 2007).

[17] A. Oksman, *Optical measurement techniques for paper and print quality evaluation*, PhD thesis (University of Joensuu, Joensuu, Finland, 2008).

[18] K. Myller, K.-E. Peiponen, and R. Silvennoinen, "Two-dimensional map of gloss of plastics measured by diffractive-element-based glossmeter," *Opt. Eng.* **42,** 3194–3197 (2003).

[19] R. Silvennoinen, K. Myller, K.-E. Peiponen, J. Salmi, and E. Pääkkönen, "Diffractive optical sensor for gloss difference of injection molded plastic products," *Sens. Actuators, A* **112,** 74–79 (2004).

[20] M. Juuti, B. van Veen, K.-E. Peiponen, J. Ketolainen, V. Kalima, R. Silvennoinen, and T. Pakkanen, "Local and average gloss from flat-faced sodium chloride tablets," *AAPS PharmSciTech* **7,** E43–E48 (2006).

[21] M. Juuti, H. Tuononen, T. Prykäri, V. Kontturi, M. Kuosmanen, E. Alarousu, J. Ketolainen, R. Myllylä, and K.-E. Peiponen, "Optical and terahertz measurement techniques for flat-faced pharmaceutical tablets: a case study of gloss, surface roughness and bulk properties of starch acetate tablets," *Meas. Sci. Technol.* **20,** 015301 (2009).

[22] K. Myller, M. Juuti, K.-E. Peiponen, R. Silvennoinen, and E. Heikkinen, "Quality inspection of metal surfaces by diffractive optical element-based glossmeter," *Precis. Eng.* **30,** 443–447 (2006).

[23] K. Myller, R. Silvennoinen, and K.-E. Peiponen, "Gloss inspection of metallic products by diffractive optical element based sensor," *Opto-Electron. Rev.,* **11,** 35–38 (2003).

[24] K.-E. Peiponen and M. Juuti, "Statistical parameters for gloss evaluation," *Appl. Phys. Lett.* **88,** 071104 (2006).

[25] M. Juuti, H. Koivula, M. Toivakka, and K.-E. Peiponen, "A diffractive gloss meter for local gloss measurement of papers and prints," *Tappi J.* **7,** 27–32 (2008).

[26] R. Silvennoinen, M. Juuti, H. Koivula, M. Toivakka, and K.-E. Peiponen, "Diffractive glossmeter for measurement of dynamic gloss of prints," *TAGA Journal* **4** (2008).

[27] C.-M. Tåg, M. Juuti, K.-E. Peiponen, and J. Rosenholm, "Print mottling: Solid-liquid adhesion related to optical appearance," *Colloids Surf., A* **317,** 658–665 (2008).

[28] M. Juuti, T. Prykäri, E. Alarousu, H. Koivula, M. Myllys, A. Lähteelä, M. Toivakka, J. Timonen, R. Myllylä, and K.-E. Peiponen, "Detection of local specular gloss and surface roughness from black prints," *Colloids Surf., A* **299,** 101–108 (2007).

[29] M. Juuti, V. Kalima, T. Pakkanen, and K.-E. Peiponen, "A novel method to measure and analyse delta gloss by diffractive glossmeter," *Meas. Sci. Technol.* **18,** L5–L8 (2007).

[30] K.-E. Peiponen, E. Alarousu, M. Juuti, R. Silvennoinen, A. Oksman, R. Myllylä, and T. Prykäri, "Diffractive-optical-element-based glossmeter and low coherence interferometer in assessment of local surface quality of paper," *Opt. Eng.* **45,** 043601 (2006).

[31] T. Kaplas, K. Laitinen, T. Moilanen, Y. Tolonen, K. Albrecht, and R. Silvennoinen, "Optical sensing of parameters crucial for japanese woodblock print making," *Opt. Rev.* **17,** 252–256 (2010).

[32] M. Juuti, K.-E. Peiponen, A. Obraztsov, R. Silvennoinen, and K. Myller, "A glossmeter for inspection of surface quality of low gloss nano-carbon surfaces," *Opt. Mater.* **29,** 1719–1722 (2007).

[33] A. Oksman, M. Juuti, and K.-E. Peiponen, "Statistical parameters and analysis of local contrast gloss," *Opt. Express* **16,** 12415–12422 (2008).

[34] A. Oksman, M. Juuti, and K.-E. Peiponen, "Sensor for the detection of local contrast gloss of products," *Opt. Lett.* **33,** 654–656 (2008).

[35] A. Oksman, M. Juuti, and K.-E. Peiponen, "Visibility map for print quality assessment by means of a diffractive optical element based glossmeter," *Meas. Sci. Technol.* **18,** 2185–2188 (2007).

[36] M. Juuti, H. Tuononen, A. Penttilä, K. Myller, K. Lumme, and K.-E. Peiponen, "Spectral properties and surface uniformity of black glass gloss reference," *Opt. Eng.* **48,** 033603 (2009).

[37] R. Silvennoinen, K.-E. Peiponen, J. Räsänen, M. Sorjonen, E. Keränen, T. Eiju, K. Tenjimbayashi, and K. Matsuda,

"Diffractive element in optical inspection of paper," *Opt. Eng.* **37,** 1482–1487 (1998).

[38] M. Sorjonen, A. Jääskeläinen, K.-E. Peiponen, and R. Silvennoinen, "On the assessment of the surface quality of black print paper by use of a diffractive optical-element-based sensor," *Meas. Sci. Technol.* **11,** N85–N88 (2000).

[39] J. Palviainen, M. Sorjonen, R. Silvennoinen, and K.-E. Peiponen, "Optical sensing of colour print on paper by a diffractive optical element," *Meas. Sci. Technol.* **13,** N31–N37 (2002).

[40] A. Oksman, R. Silvennoinen, K.-E. Peiponen, M. Avikainen, and H. Komulainen, "A diffractive optical element based machine vision system for local optical inspection of compressed paper," *Opto-Electron. Rev.* **13,** 39–42 (2005).

[41] K.-E. Peiponen, R. Silvennoinen, J. Räsänen, K. Matsuda, and V. Tanninen, "Optical coating inspection of pharmaceutical tablets by diffractive element," *Meas. Sci. Technol.* **8,** 815818 (1997).

[42] R. Silvennoinen, K.-E. Peiponen, P. Laakkonen, J. Ketolainen, E. Suihko, P. Paronen, J. Räsänen, and K. Matsuda, "On the optical inspection of the surface quality of pharmaceutical tablets," *Meas. Sci. Technol.* **8,** 550–554 (1997).

[43] S.-P. Simonaho and R. Silvennoinen, "Sensing of wood density by laser light scattering pattern and diffractive optical element based sensor," *J. Opt. Technol.* **73,** 170–174 (2006).

[44] R. Silvennoinen, P. Wahl, and J. Vidot, "Inspection of orientation of micro fibres in dried wood by a diffractive optical element," *Opt. Lasers Eng.* **33,** 29–38 (2000).

[45] R. Silvennoinen, J. Palviainen, S. Kellomäki, H. Peltola, and K. Sauvala, "Detection of wood density by using a DOE sensor," *Wood Sci. Technol.* **36,** 157–162 (2002).

[46] J. Palviainen and R. Silvennoinen, "Inspection of wood density by spectrophotometry and a diffractive optical element based sensor," *Meas. Sci. Technol.* **12,** 345–352 (2001).

[47] A. Jääskeläinen, R. Silvennoinen, K.-E. Peiponen, and J. Räty, "On measurement of complex refractive index of liquids by diffractive element-based sensor," *Optics Communications* **178,** 53–57 (2000).

[48] R. Silvennoinen, K.-E. Peiponen, and J. Räty, "Detection of refractive index change of liquids by diffractive element based sensor," *Opt. Rev.* **6,** 68–70 (1999).

[49] J. Räsänen and K.-E. Peiponen, "On-line measurement of the thickness and optical quality of float glass with a sensor based on a diffractive element," *Appl. Opt.* **40,** 5034–5039 (2001).

[50] V. Hyvärinen, R. Silvennoinen, K.-E. Peiponen, and T. Niskanen, "Diffractive optical element based sensor for surface quality inspection of concave punches," *Eur. J. Pharm. Biopharm.* **49,** 167–169 (2000).

[51] V. Hyvärinen, K.-E. Peiponen, R. Silvennoinen, P. Raatikainen, P. Paronen, and T. Niskanen, "Optical inspection of punches: flat surfaces," *Eur. J. Pharm. Biopharm.* **49,** 87–90 (2000).

[52] R. Silvennoinen, V. Vetterl, S. Hasoň, M. Silvennoinen, K. Myller, J. Vaněk, and L. Cvrček, "Optical sensing of attached fibrinogen on carbon doped titanium surfaces," *Advances in Optical Technology* **2010,** 1–8 (2010).

[53] R. Silvennoinen, S. Hasoň, V. Vetterl, N. Penttinen, M. Silvennoinen, K. Myller, P. Černochová, S. Bartková, P. Prachár, and L. Cvrček, "Diffractive-optics-based sensor as a tool for detection of biocompatibility of titanium and titanium-doped hydrocarbon samples," *Appl. Opt.* **49,** 5583–5591 (2010).

[54] K. Myller, K.-E. Peiponen, R. Silvennoinen, J.-P. Tarvainen, J. Rainio, and S. Soinila-Oksanen, "Glossmeter for detection of gloss and wear of concave glazed ceramic products," *DKG* **81,** E39–E42 (2004).

[55] R. Silvennoinen, J. Räsänen, M. Savolainen, K.-E. Peiponen, J. Uozumi, and T. Asakura, "On simultaneous optical sensing of local curvature and roughness of metal surface," *Sens. Actuators, A* **51,** 117–123 (1996).

[56] J. Christie, "An instrument for the geometric attributes of metallic appearance," *Appl. Opt.* **8,** 1777–1785 (1969).

[57] I. Ariño, U. Kleist, L. Mattsson, and M. Rigdahl, "On the relation between surface texture and gloss of injection-molded pigmented plastic," *Polym. Eng. Sci.* **45,** 1343–1356 (2005).

[58] S. Ignell, U. Kleist, and M. Rigdahl, "On the relations between color, gloss, and surface texture in injection-molded plastics," *COLOR research and applications* **34,** 291–300 (2009).

[59] S. Heintze, M. Forjanic, and V. Rousson, "Surface roughness and gloss of dental materials as a function of force and polishing time in vitro," *Dent. Mater.* **22,** 146–165 (2006).

[60] D. Desjumaux, D. Bousfield, T. Glatter, and R. van Gilder, "The influence of latex type and concentration on ink gloss dynamics," *Prog. Org. Coat.* **38,** 89–95 (2000).

[61] M. Lindstrand, "Instrumental gloss characterization-in the light of visual evaluation: a review," *J. Imaging Sci. Tech.* **49,** 61–70 (2005).

[62] M. Lindstrand, "An angularly and spatially resolved reflectometer for a perceptually adequately characterization of gloss," *J. Imaging Sci. Tech.* **49,** 71–84 (2005).

[63] M.-C. Béland and J. Bennett, "Effect of local microroughness on the gloss uniformity of printed paper surface," *Appl. Opt.* **39,** 2719–2726 (2000).

[64] M. MacGregor, "A review of the topographical causes of gloss variation and the effect on perceived print quality," Proc. Hansol Symposium (2000).

[65] M.-C. Béland, S. Lindberg, and P.-Å. Johansson, "Optical measurement and perception of gloss quality of printed matte-coated paper," *J. Pulp Pap. Sci.* **26,** 120–123 (2000).

[66] N. Pauler, *Paper Optics* (AB Lorentzen and Wettre, Kista, 2002).

[67] H. Kipphan, *Handbook of Print Media: Technologies and Production Methods* (Springer, Berlin, 2001).

[68] V. Briones, J. M. Aguilera, and C. Brown, "Effect of surface topography on color and gloss of chocolate samples," *J. Food Eng.* **77,** 776–783 (2006).

[69] A. Mizrach, R. Lu, and M. Rubino, "Gloss evaluation of curved-surface fruits and vegetables," *Food Bioprocess Technol.* **2,** 300–307 (2008).

[70] F. Mendoza, P. Dejmek, and J. Aquilera, "Gloss measurement of raw agricultural products using image analysis," *Food Res. Int.* **43,** 18–25 (2010).

[71] G. W. A. Nussinovitch and E. Mey-Tal, "Gloss of fruits and vegetables," *Lebensmittel-Wissenschaft und-Technologie* **29,** 184–186 (1996).

[72] C. Pastor, J. Santamaría, A. Chriralt, and J. Aguilera, "Gloss and colour of dark chocolate during storage," *Food Sci. Technol. Int.* **13,** 27–34 (2007).

[73] S. Jha, T. Matsuoka, and K. Miyauchi, "PH-Postharvest technology: surface gloss and weight of eggplant during storage," *Biosystems Eng.* **81,** 407–412 (2002).

[74] T. Trezza and J. Krochta, "Specular reflection, gloss, roughness and surface heterogeneity of biopolymer coatings," *J. Appl. Polym. Sci.* **79,** 2221–2229 (2001).

[75] "Paper and board - Measurement of specular gloss - Part 1: 75 degree gloss with a converging beam, TAPPI method," *International Organization for Standardization, Geneve, Switzerland* (1999).

[76] "Paper and board - Measurement of specular gloss - Part 2: 75 degree gloss with a parallel beam, DIN method," *International Organization for Standardization, Geneve, Switzerland* (2003).

[77] "Paper and board - Measurement of specular gloss - Part 3: 20 degree gloss with a converging beam, TAPPI method," *International Organization for Standardization, Geneve, Switzerland* (2004).

[78] W. Budde, "The calibration of gloss reference standards," *Metrologia* **16,** 89–93 (1980).

[79] M. E. Nadal and A. Thompson, "New primary standard for specular gloss measurements," *J. Coating Technol.* **72,** 61–66 (2000).

[80] B. Anderson and J. Kim, "Image statistics do not explain the perception of gloss and lightness," *J Vis* **9,** 1–17 (2009).

[81] M. Wijntjes and S. Pont, "Illusory gloss on lambertian surface," *J Vis* **10,** 1–12 (2010).

[82] N. Elton and J. Day, "A reflectometer for the combined measurement of refractive index, microroughness, macroroughness and gloss of low-extinction surface," *Meas. Sci. Technol.* **20,** 025309 (2009).

[83] R. Alexander-Katz and R. Barrera, "Surface correlation effects on gloss," *J. Polym. Sci. Pol. Phys.* **36,** 1321–1334 (1998).

[84] I. Simonsen, Å. G. Larsen, E. Andreassen, E. Ommundsen, and K. Nord-Varhaug, "Estimation of gloss from rough surface parameters," *Phys. Stat. Sol. b* **242,** 2995–3000 (2005).

[85] P. Rastogi, *Optical Measurement Techniques and Applications* (Artech House, Boston, 1997).

[86] L. Gate, W. Windle, and M. Hine, "The relationship between gloss and surface microtexture of coatings," *Tappi J.* **56,** 61–65 (1973).

[87] C. Poon and B. Bhusban, "Comparison of surface roughness measurements by stylus profiler, AFM and non-contact optical profiler," *Wear* **190,** 76–88 (1995).

[88] J. Bennett and J. Dancy, "Stylus profiling instrument for measuring statistical properties of smooth optical surfaces," *Appl. Opt.* **20,** 1785–1802 (1981).

[89] S. Whitehead, A. Shearer, D. Watts, and N. Wilson, "Comparison of two stylus methods for measuring surface texture," *Dent. Mater.* **15,** 79–86 (1999).

[90] K. Stout and L. Blunt, "Nanometres to micrometres: three-dimensional surface measurement on bio-engineering," *Surf. Coat. Technol.* **71,** 69–81 (1995).

[91] R.-S. Lu and G. Tian, "On-line measurement of surface roughness by laser light scattering," *Meas. Sci. Technol.* **17,** 1496–1502 (2006).

[92] W. Wang, P. Wong, J. Luo, and Z. Zhang, "A new optical technique for roughness measurement on moving surface," *Tribol. Int.* **31,** 281–287 (1998).

[93] P. Wong and K. Li, "In-process roughness measurement on moving surfaces," *Opt. Laser Technol.* **31,** 543–548 (1999).

[94] D. Léger, E. Mathieu, and J. Perrin, "Optical surface roughness determination using speckle correlation technique," *Appl. Opt.* **14,** 872–877 (1975).

[95] D. Léger and J. Perrin, "Real-time measurement of surface roughness by correlation of speckle patterns," *J. Opt. Soc. Am.* **66,** 1210–1217 (1976).

[96] U. Person, "Surface roughness measurement on machined surfaces using angular speckle correlation," *J. Mater. Process. Technol.* **180,** 233–238 (2006).

[97] M. Rebollo, E. Hogert, J. Albano, C. Raffo, and N. Gaggioli, "Correlation between roughness and porosity in rocks," *Opt. Laser Technol.* **28,** 21–23 (1996).

[98] S. Toh, C. Quan, K. Woo, C. Tay, and H. Shang, "Whole field surface roughness measurement by laser speckle correlation technique," *Opt. Laser Technol.* **33,** 427–434 (2001).

[99] K.-E. Peiponen, R. Myllylä, and A. Priezzhev, *Optical measurement techniques : innovations for industry and the life sciences* (Springer, Berlin, 2009).

[100] R. Erf, *Speckle Metrology* (Academic Press, London, 1978).

[101] J. Goodman, "Statistical Properties of Laser Speckle Patterns," *Laser Speckle and Related Phenomena*, J. Dainty, Editor, 9-75 (Springer-Verlag, Berlin, Germany,1975).

[102] M. Draijer, E. Hondebrink, T. van Leeuwen, and W. Steenbergen, "Review of laser speckle contrast techniques for visualizing tissue perfusion," *Lasers Med. Sci.* **24,** 639–651 (2009).

[103] H. Nitta and T. Asakura, "Method for measuring mean particle size of the bulk powder using speckle patterns," *Appl. Opt.* **30,** 4854–4858 (1991).

[104] D. Death, J. Eberhardt, and C. Rogers, "Transparency effects on powder speckle decorrelation," *Opt. Express* **6,** 202–212 (2000).

[105] S. Ulyanov and V. Tuchin, "Use of low-coherence speckled speckles for bioflow measurements," *Appl. Opt.* **39,** 6385–6389 (2000).

[106] R. Silvennoinen, V. Hyvärinen, P. Raatikainen, and K.-E. Peiponen, "Dynamic laser speckle pattern in monitoring of local deformation of tablet surface after compression," *Int. J. Pharm.* **199,** 205–208 (2000).

[107] S. Yuan, A. Devor, D. Boas, and A. Dunn, "Determination of optimal exposure time for imaging of blood flow changes with laser speckle contrast imaging," *Appl. Opt.* **44,** 1823–1830 (2005).

[108] E. Hecht, *Optics* (Addison Wesley, San Francisco, 2002).

[109] E. Palik, *Handbook of Optical Constant of Solids* (Academic Press, Orlando, 1985).

[110] J. Räsänen, M. Savolainen, R. Silvennoinen, and K.-E. Peiponen, "Optical sensing of surface roughness and waviness by a computer-generated hologram," *Opt. Eng.* **34,** 2574–2580 (1995).

[111] M. Nieto-Vesperinas, *Scattering and Diffraction in Physical Optics* (Wiley, New York, 1991).

[112] J. Latta, "Computer-based analysis of hologram imagery and aberrations. I: hologram types and their nonchramatic aberrations," *Appl. Opt.* **10,** 599–608 (1971).

[113] J. Latta, "Computer-based analysis of hologram imagery and aberrations II: aberrations induced by a wavelength shift," *Appl. Opt.* **10,** 609–618 (1971).

[114] A. Cook, *Advances in on-line appearance measurement* (Pergamon Press, Oxford, 1980).

[115] Y. Shibata, Y. Asano, and K. Kurita, "On-line glossmeter for stainless steel sheets," *Optical Techiques for Industrial Inspection*, P. Cielo, Editor, Proc. SPIE 665, 25-31 (1986).

[116] R. Xu, P. Fleming, and A. Pekarovicova, "The effect of inkjet paper roughness on print gloss," *J. Imaging Sci. Technol.* **49,** 660–666 (2005).

[117] J. Järnström, P. Ihalainen, K. Backfolk, and J. Peltonen, "Roughness of pigment coatings and its influence on gloss," *Appl. Surf. Sci.* **254,** 5741–5749 (2008).

[118] S. Jeon and D. Bousfield, "Print gloss development with controlled coating structures," *J. Pulp Pap. Sci.* **30,** 99–104 (2004).

[119] J. Preston, A. Hiorns, N. Elton, and G. Ström, "Application of imaging reflectometry to studies of print mottle on commercially printed coated papers," *Tappi J.* **7,** 11–18 (2008).

[120] M. Karathanasis and A. Fogden, "The concept of critical ink setting time and its relation to print gloss -Influence of latex binder," *Nord Pulp Pap. Res. J.* **18,** 145–149 (2003).

[121] M. MacGregor and P.-Å. Johansson, "Submillimeter gloss variations in coated paper. Part 1: the gloss imaging equipment and analytical techniques," *Tappi J.* **73,** 161–168 (1990).

[122] M. MacGregor and P.-Å. Johansson, "Submillimeter gloss variations in coated paper. Part 2: studying "orange peel" gloss effects in a lightweight coated paper," *Tappi J.* **74,** 187–194 (1991).

[123] J. Arney, L. Ye, J. Wible, and T. Oswald, "Analysis of paper gloss," *J. Pulp Pap. Sci.* **32,** 19–23 (2006).

[124] N. Elton and J. Preston, "Polarized light reflectometry for studies of paper coating structure. Part 1. Method and instrumentation," *Tappi J.* **5,** 8–15 (2006).

[125] N. Elton and J. Preston, "Polarized light reflectometry for studies of paper coating structure Part 2. Application to coating structure gloss and porosity," *Tappi J.* **5,** 10–16 (2006).

[126] T. Glatter and D. Bousfield, "Print gloss development on a model substrate," *Tappi J.* **80,** 125–132 (1997).

[127] S.-S. Lin, K. Yemelyano, E. Pugh, and N. Engheta, "Polarization-based and specular-reflection-based noncontact latent fingerprint imaging and lifting.," *J. Opt. Soc. Am. A* **23,** 2137–2153 (2006).

[128] S. K. Dubey, T. Anna, C. Shakher, and D. Mehta, "Fingerprint detection using full-field swept-source optical coherence tomography," *Appl. Phys. Lett.* **91,** 181106 (2007).

[129] S. Chang, Y. Cheng, K. Larin, Y. Mao, S. Sherif, and C. Flueraru, "Optical coherence tomography used for security and fingerprint-sensing applications," *IET Image Proc.* **2,** 48–58 (2008).

[130] A. Bossen, R. Lehmann, and C. Meier, "Internal fingerprint identification with optical coherence tomography," *IEEE Photonics Technol. Lett.* **22,** 507–509 (2010).

[131] E. Emmons, A. Tripathi, J. Guichheteau, S. Christensen, and A. Fountain, "Raman chemical imaging of explosive-contamined fingerprints," *Appl. Spectrosc.* **63,** 1197–1203 (2009).

[132] B. J. Kang, K. Park, J.-H. Yoo, and J. N. Kim, "Multimodal biometric method that combines veins prints, and shape of a finger," *Opt. Eng.* **50,** 017201 (2011).

Kalle Kuivalainen

Glossmeters for the measurement of glos from flat and curved objects

This thesis deals with the development of a diffractive optical element (DOE) based glossmeter (DOG). It includes flat and curved surface gloss measurement. The flat surface gloss inspection includes off-line and on-line gloss measurements with new generations DOGs. Also a single sensor which can measure both gloss and surface roughness is also presented. The DOGs for the curved surface were modified from the DOGs used for flat surface gloss inspection and two statistical gloss parameters for the curved surface gloss evaluation are presented in this thesis. The curved surface gloss measurement also includes one application where a latent fingerprint was detected on a ballpoint pen surface with the DOG.

UNIVERSITY OF
EASTERN FINLAND

Publications of the University of Eastern Finland
Dissertations in Forestry and Natural Sciences

ISBN: 978-952-61-0524-6 (printed)
ISSNL: 1798-5668
ISSN: 1798-5668